Molecular Meccano, Part 44[+]

Photoactive Azobenzene-Containing Supramolecular Complexes and Related Interlocked Molecular Compounds

Masumi Asakawa,[b] Peter R. Ashton,[b] Vincenzo Balzani,*[a] Christopher L. Brown,[b] Alberto Credi,[a] Owen A. Matthews,[b] Simon P. Newton,[b] Françisco M. Raymo,[b] Andrew N. Shipway,[b] Neil Spencer,[b] Andrew Quick,[c] J. Fraser Stoddart,*[b] Andrew J. P. White,[c] and David J. Williams*[c]

Abstract: Two acyclic and three macrocyclic polyethers, three [2]catenanes, and one [2]rotaxane, each containing one 4,4′-azobiphenoxy unit, have been synthesized. In solution, the azobenzene-based acyclic polyethers are bound by cyclobis(paraquat-*p*-phenylene)—a tetracationic cyclophane—in their *trans* forms only. On irradiation ($\lambda = 360$ nm) of an equimolar solution of the tetracationic cyclophane host and one of the guests containing a *trans*-4,4′-azobiphenoxy unit, the *trans* double bond isomerizes to its *cis* form and the supramolecular complex dissociates into its molecular components. The *trans* isomer of the guest and, as a result, the complex are reformed, either by irradiation ($\lambda =$ 440 nm) or by warming the solution in the dark. Variable temperature ^{1}H NMR spectroscopic investigations of the [2]catenanes and the [2]rotaxane revealed that, in all cases, the 4,4′-azobiphenoxy unit resides preferentially alongside the cavities of their tetracationic cyclophane components, which are occupied either by a 1,4-dioxybenzene or by a 1,5-dioxynaphthalene unit. In the acyclic and macrocyclic polyethers containing 1,4-dioxybenzene or 1,5-dioxynaphthalene chromophoric groups and a 4,4′-azobiphenoxy moiety, the fluorescence of the former units is quenched by the latter. Fluorescence quenching is accompanied by photosensitization of the isomerization. The rate of the energy-transfer process is different for *trans* and *cis* isomers. In the [2]rotaxane and the [2]catenanes, the photoisomerization is quenched to an extent that depends on the specific structure of the compound. Only in one of the three [2]catenanes and in the [2]rotaxane was an efficient photoisomerization ($\lambda = 360$ nm) from the *trans* to the *cis* isomer of the 4,4′-azobiphenoxy unit observed. Single crystal X-ray structural analysis of one of the [2]catenanes showed that, in the solid state, the 4,4′-azobiphenoxy unit in the macrocyclic polyether component also resides exclusively alongside. The cavity of the tetracationic cyclophane component of the [2]catenane is filled by a 1,5-dioxynaphthalene unit, and infinite donor–acceptor stacks between adjacent [2]catenanes are formed in the crystal. These supramolecular complexes and their mechanically interlocked molecular counterparts can be regarded as potential photoactive nanoscale devices.

Keywords: catenanes · molecular devices · molecular recognition · rotaxanes · template synthesis

[a] Prof. V. Balzani, Dr A. Credi
Dipartimento di Chimica G. Ciamician, Università di Bologna
Via Selmi 2, I-40126 Bologna, Italy
Fax: (+390) 51-259456
E-mail: vbalzani@ciam.unibo.it

[b] Prof. J. F. Stoddart,[+] Dr M. Asakawa, Dr C. L. Brown, Dr O. A. Matthews, Dr S. P. Newton, Dr F. M. Raymo,[+] Dr A. N. Shipway, Dr N. Spencer, P. R. Ashton
School of Chemistry, University of Birmingham
Edgbaston, Birmingham, B15 2TT (UK)

[c] Prof. D. J. Williams, Dr A. Quick, Dr A. J. P. White
Department of Chemistry, Imperial College
South Kensington, London, SW7 2AY (UK)
Fax: (+44) 171-594-5835

[+] Current address:
Department of Chemistry and Biochemistry, University of California
Los Angeles, 405 Hilgard Avenue, Los Angeles
CA 90095-1569 (USA)
Fax: (+1) 310-206-1843
E-mail: stoddart@chem.ucla.edu

[+] Part 43: P. R. Ashton, M. C. T. Fyfe, S. K. Hickingbottom, J. F. Stoddart, A. J. P. White, D. J. Williams, *J. Chem. Soc. Perkin Trans. 2* **1998**, 2117–2128.

0947-6539/99/0503-0860 $ 17.50+.50/0

Introduction

trans-Azobenzene is thermodynamically stable under normal conditions, but isomerizes[1] to the *cis* isomer upon exposure to UV light ($\lambda = 310-370$ nm). On further irradiation ($\lambda >$ 380 nm) and/or by heating, *cis*-azobenzene isomerizes back to the *trans* isomer, and the process can be repeated indefinitely. Thus, azobenzene can be considered[1b, 2] as a molecular-sized switch that can be interconverted reversibly from an ON state (e.g., the *trans* isomer) to an OFF state (e.g., the *cis* isomer) by external stimuli (e.g., photochemical and/or thermal), that is, an input from the macroscopic world generates a response at the molecular (microscopic) level. Indeed, a number of molecular and supramolecular systems, incorporating one or more azobenzene units, have already been designed and realized,[1, 3] the ultimate goal being to control their properties reversibly by switching the azobenzene unit(s) from the *trans* to the *cis* isomer(s) and vice versa.

The π-electron-deficient host cyclobis(paraquat-*p*-phenylene) **1**·4PF$_6$ binds[4] π-electron-rich acyclic guests to give pseudorotaxane geometries both in solution and in the solid state. The noncovalent bonding interactions responsible for the complexation are [C–H···O] hydrogen bonds, π–π stacking, and [C–H···π] interactions between the complementary recognition sites incorporated within the host and the guest. In order to control reversibly the molecular-recognition event by external stimuli, we envisaged the possibility of introducing azobenzene units into the π-electron-rich components of such supramolecular complexes, as well as into their related mechanically interlocked molecules.[5] Here, we report i) the synthesis of two π-electron-rich azobenzene-containing guests that are bound by **1**·4PF$_6$ in their *trans* form only, ii) the template-directed syntheses of three [2]catenanes and a [2]rotaxane containing in all cases one azobenzene unit[6] in their π-electron-rich components, iii) variable temperature ^{1}H-NMR spectroscopic investigations of the dynamic processes associated with these mechanically interlocked molecules in solution, iv) the photophysical characterization of all the azobenzene-containing compounds, and v) single crystal X-ray structural analyses of one complex, as well as of one [2]catenane and of its free macrocyclic polyether component.

Results and Discussion

Synthesis: The syntheses are illustrated in Schemes 1–4. Alkylation (Scheme 1) of **2** with **3**, followed by tosylation of the resulting alcohol **4**, gave **5**. Reaction of **6** with **7** or **5** afforded the corresponding acyclic polyethers **8** or **9**, respectively. Macrocyclization (Scheme 2) of **6** and **10** or **11**, under high dilution conditions, gave the macrocyclic polyethers **12** or **13**, respectively. Reaction of **14**·2PF$_6$ with **15** in the presence of either **12** or **13** yielded the [2]catenanes **16**·4PF$_6$ or **17**·4PF$_6$, respectively, after counterion exchange. Alkylation (Scheme 3) of **6** with **18** gave the diol **19**, which was converted into the bistosylate **20**. Macrocyclization of **20** and **21** under high dilution conditions afforded the macrocyclic polyether **22**. Reaction of **14**·2PF$_6$ with **15** in the presence of **22** gave the [2]catenane **23**·4PF$_6$, after counterion exchange. The alcohol **24** was converted (Scheme 4) into the tosylate **25**, which was

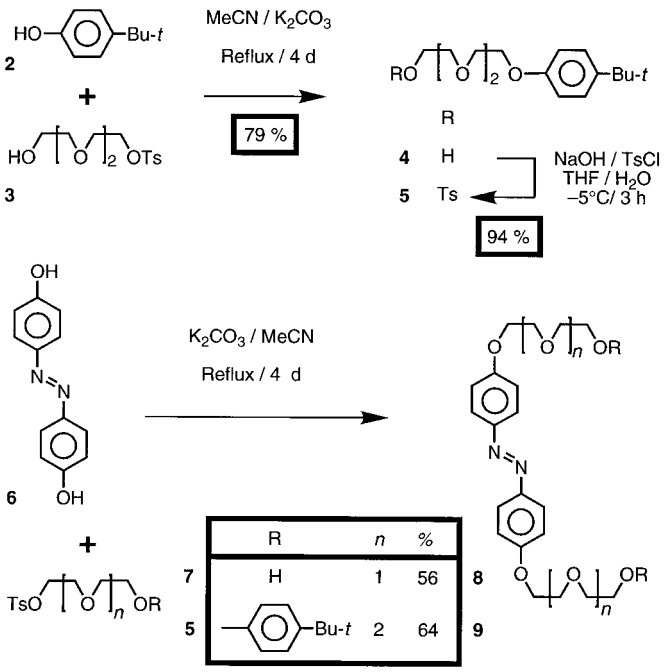

Scheme 1. Synthesis of the azobenzene-containing acyclic polyethers **8** and **9**.

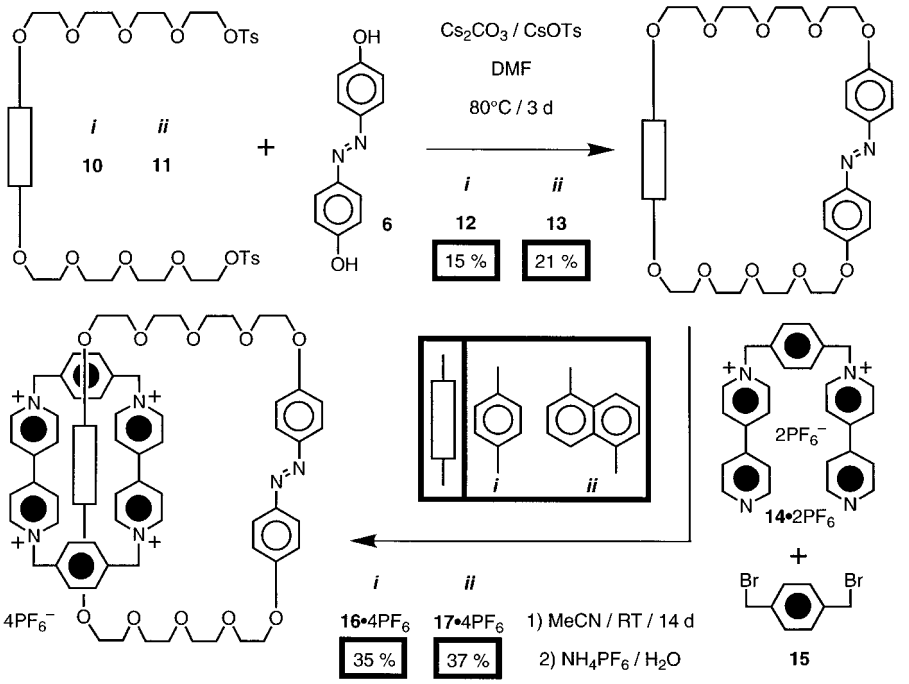

Scheme 2. Template-directed syntheses of the azobenzene-containing [2]catenanes **16**·4PF$_6$ and **17**·4PF$_6$.

  0947-6539/99/0503-0861 $ 17.50+.50/0

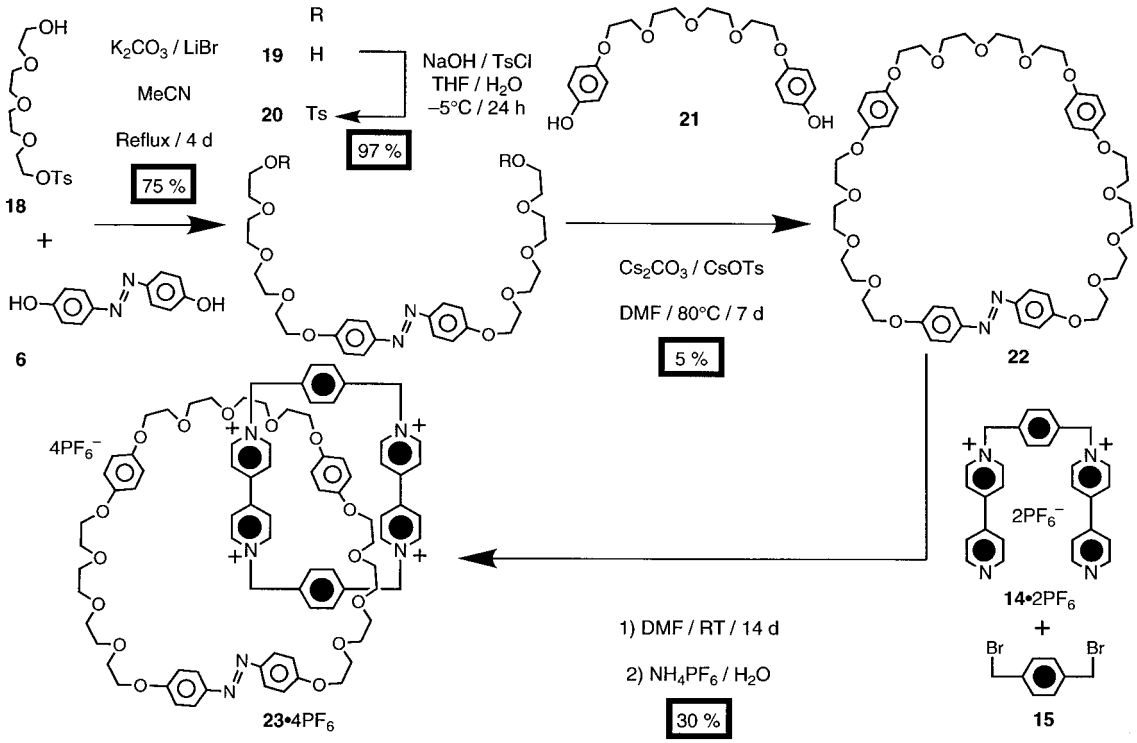

Scheme 3. Template-directed synthesis of the azobenzene-containing [2]catenane **23**·4PF$_6$.

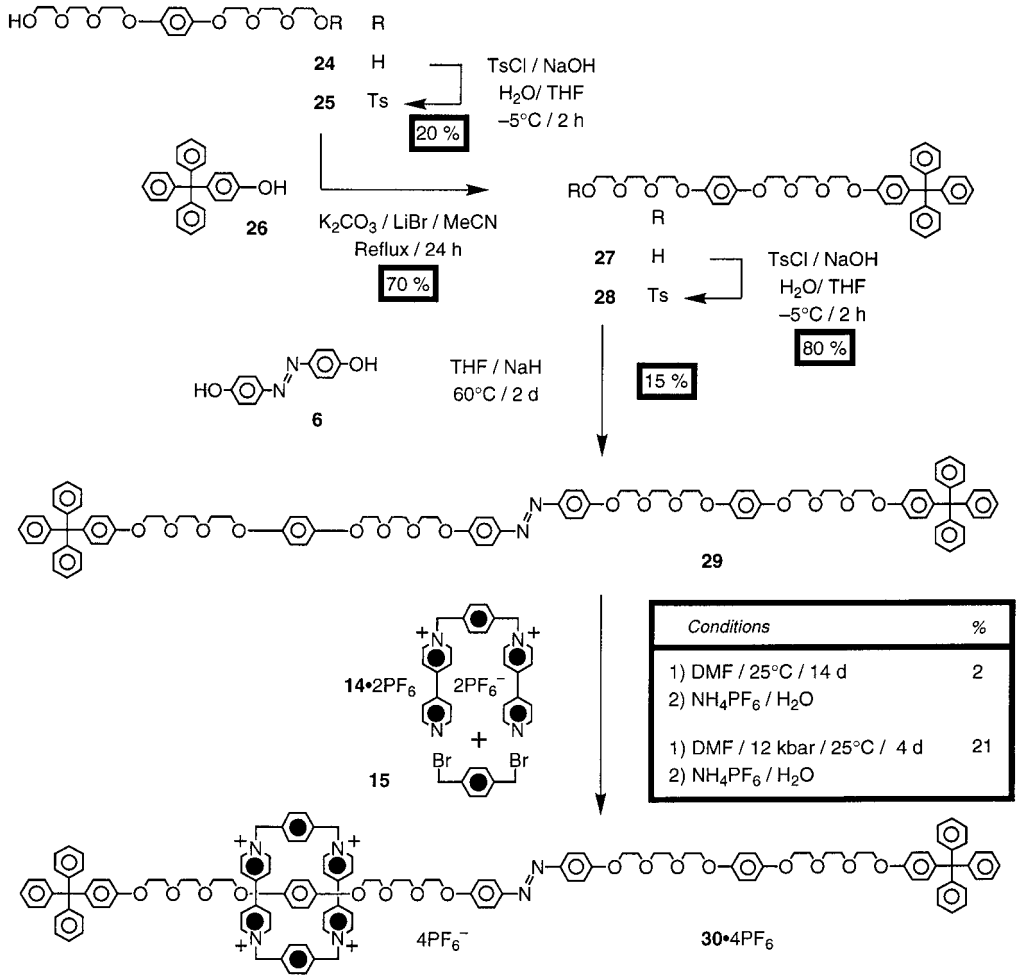

Scheme 4. Template-directed synthesis of the azobenzene-containing [2]rotaxane **30**·4PF$_6$.

0947-6539/99/0503-0862 $ 17.50+.50/0 *Chem. Eur. J.* **1999**, *5*, No. 3

treated with **26** to afford the alcohol **27**. Tosylation of **27**, followed by the reaction of the resulting tosylate **28** with **6**, gave the dumbbell-shaped compound **29**. Reaction of **14**·$2PF_6$ with **15** in DMF at ambient temperature and pressure in the presence of **29** afforded the [2]rotaxane **30**·$4PF_6$ in 2% yield, after counterion exchange. When the same reaction was performed under ultrahigh pressure (12 kbar) conditions, the yield of **30**·$4PF_6$ raised to 21%.

^{1}H NMR spectroscopy: The *trans* isomers of the azobenzene-based acyclic polyethers **8** and **9** are bound in solution by the tetracationic cyclophane **1**·$4PF_6$ with 1:1 stoichiometries and pseudorotaxane geometries (Figure 1).[7] In the case of *trans*-**8**, the 1:1 complex and the free host and guest are in fast exchange on the ^{1}H NMR timescale in CD_3CN at 298 K. Hence, averaged signals are observed in the ^{1}H NMR spectrum of an equimolar solution of *trans*-**8** and **1**·$4PF_6$. The resonances of the protons attached to the azobenzene unit of *trans*-**8** shift ($\Delta\delta \cong -1.0$ ppm) upon complexation as a result of shielding effects exerted by the sandwiching bipyridinium units. From the observation of the change in chemical shift of these protons upon dilution of an equimolar solution of *trans*-**8** and **1**·$4PF_6$ in CD_3CN at 298 K, the association constant (K_a) of the corresponding 1:1 complex was determined ($K_a = 469 \pm 37\ M^{-1}$, $\Delta G^\circ = -3.7 \pm 0.1$ kcal mol^{-1}). In the case of *trans*-**9**, the 1:1 complex and the free host and guest are in slow exchange on the ^{1}H NMR timescale in CD_3CN at 298 K, and separate signals for complexed and uncomplexed species are observed (Figure 2a) in the ^{1}H NMR spectrum of an equimolar solution of *trans*-**9** and **1**·$4PF_6$. By measuring the relative intensities of the resonances associated with complexed and uncomplexed species, a K_a value of $370 \pm 70\ M^{-1}$ ($\Delta G^\circ = -3.6 \pm 0.1$ kcal mol^{-1}) was determined for the 1:1 complex formed between *trans*-**9** and **1**·$4PF_6$.

After the irradiation ($\lambda = 360$ nm) of a solution of *trans*-**8** in CD_3CN for 1 h at 298 K, partial isomerization of *trans*-**8** to *cis*-**8** occurs, and the resonances of both isomers can be observed in the ^{1}H NMR spectrum in a ratio of 40:60 (*trans:cis*). In particular, the ^{1}H NMR spectrum shows the appearance of a resonance[8] centered on $\delta = 6.89$, which corresponds to the aromatic protons of *cis*-**8**. Upon addition of one molar equivalent of the tetracationic cyclophane **1**·$4PF_6$ to the solution containing both isomers, the resonances of *trans*-**8** shift dramatically, while those of *cis*-**8** remain unchanged, suggesting that the *cis* isomer is only very weakly or indeed not bound at all by the tetracationic cyclophane. After the thermal re-isomerization, the signals of *cis*-**8** disappear from the ^{1}H NMR spectrum, which shows only averaged resonances for complexed and uncomplexed *trans*-**8** and **1**·$4PF_6$. A similar effect was observed (Figure 2b) when an equimolar CD_3CN solution of *trans*-**9** and **1**·$4PF_6$ was irradiated ($\lambda =$ 360 nm) for 1 h at 298 K. Again, a resonance[8] centered on $\delta = 6.81$ for the aromatic protons of *cis*-**9** appears in the ^{1}H NMR spectrum, and the ratio between the two isomers of **9** is 40:60 (*trans:cis*). Furthermore, the ratio between uncomplexed and complexed **1**·$4PF_6$ increases in favor of the uncomplexed species, suggesting once again that the *cis* isomer of **9** is only weakly bound, or not at all, by the tetracationic cyclophane. After thermal re-isomerization, the resonances of *cis*-**9** disappear, and a ^{1}H NMR spectrum, identical to that shown in Figure 2a, is obtained. The photoinduced dethreading of the 4,4′-azobiphenoxy unit as a consequence of *trans*→*cis* isomerization has been confirmed by photochemical measurements (vide infra).

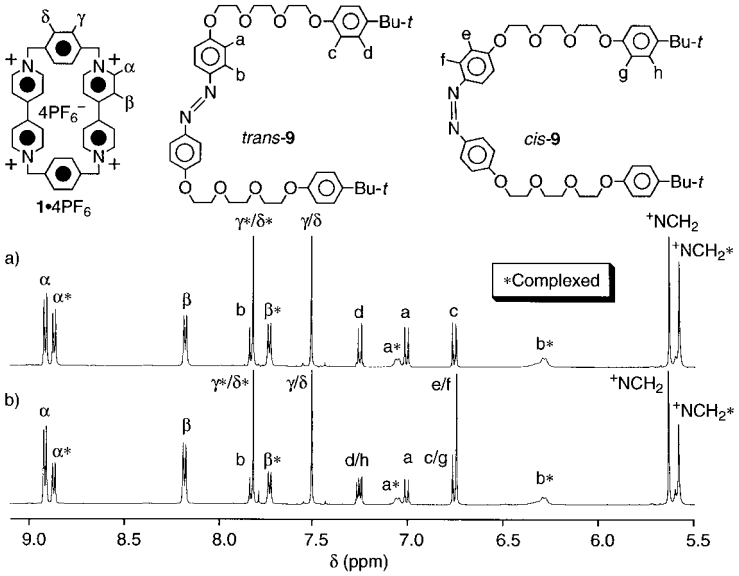

Figure 2. Partial ^{1}H NMR spectra of equimolar CD_3CN solutions of **1**·$4PF_6$ and **9** a) before and b) after irradiation ($\lambda = 360$ nm) of the solution for 1 h at 298 K.

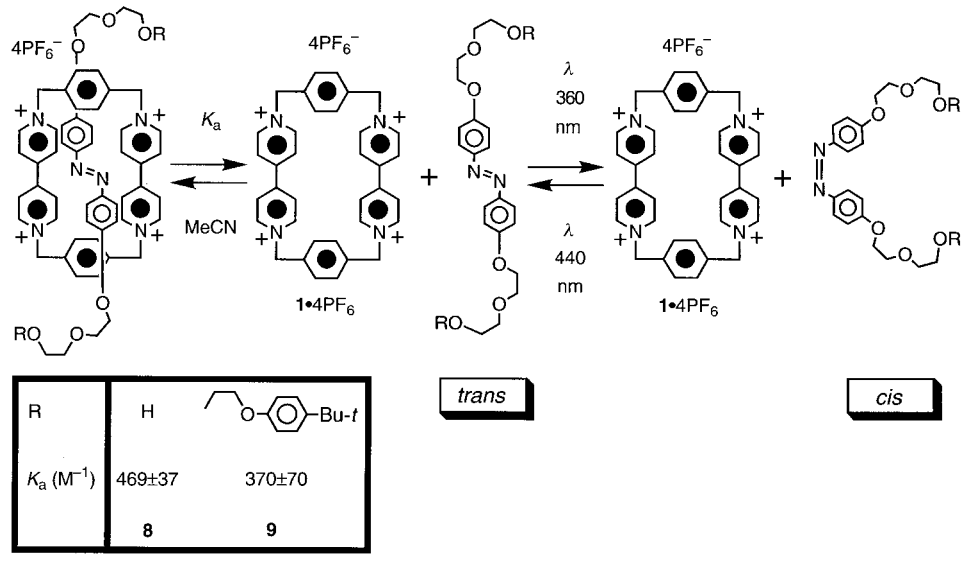

Figure 1. Complexation of the *trans* isomers of the azobenzene-based acyclic polyethers **8** and **9** by the tetracationic cyclophane **1**·$4PF_6$.

Comparison of the ^{1}H NMR spectrum of the macrocyclic

polyether **12** with that of the [2]catenane **16**·4PF_6 (Figure 3a)—both recorded in $(CD_3)_2SO$ at 370 K—shows upfield shifts for the protons attached to the 1,4-dioxybenzene ring ($\Delta\delta = -2.69$ ppm) and to the 4,4′-azobiphenoxy unit ($\Delta\delta \cong -0.25$ ppm). These changes are a result of shielding effects exerted by the bipyridinium units present in the [2]catenane and are much more pronounced for the 1,4-dioxybenzene protons, indicating that this ring is located preferentially inside the cavity of the tetracationic cyclophane component. The protons in the α and β positions, with respect to the nitrogen atoms, on the bipyridinium units give rise to sharp and well-resolved signals in the ^{1}H NMR spectrum of **16**·4PF_6, recorded in $(CD_3)_2SO$ at 370 K (Figure 3a), suggesting that the inside and alongside bipyridinium units are in fast exchange on the ^{1}H NMR timescale. On cooling a $(CD_3)_2SO$ solution of **16**·4PF_6 down, the signal corresponding to the 1,4 dioxybenzene protons becomes broad (Figure 3b) in the ^{1}H NMR spectrum and eventually merges into the baseline (Figure 3c). However, on further cooling of a $(CD_3)_2CO$ solution of **16**·4PF_6 down to 290 K, the resonance of the 1,4-dioxybenzene protons reappears (Figure 3d) at $\delta = 3.45$. These changes are accompanied by a downfield shift ($\Delta\delta \cong +0.3$ ppm) of the 4,4′-azobiphenoxy protons, suggesting that the circumrotation of the macrocyclic polyether through the cavity of the tetracationic cyclophane component becomes slow on the ^{1}H NMR timescale as the temperature is reduced, and, moreover, that the tetracationic cyclophane resides exclusively around the 1,4-dioxybenzene ring at 290 K.

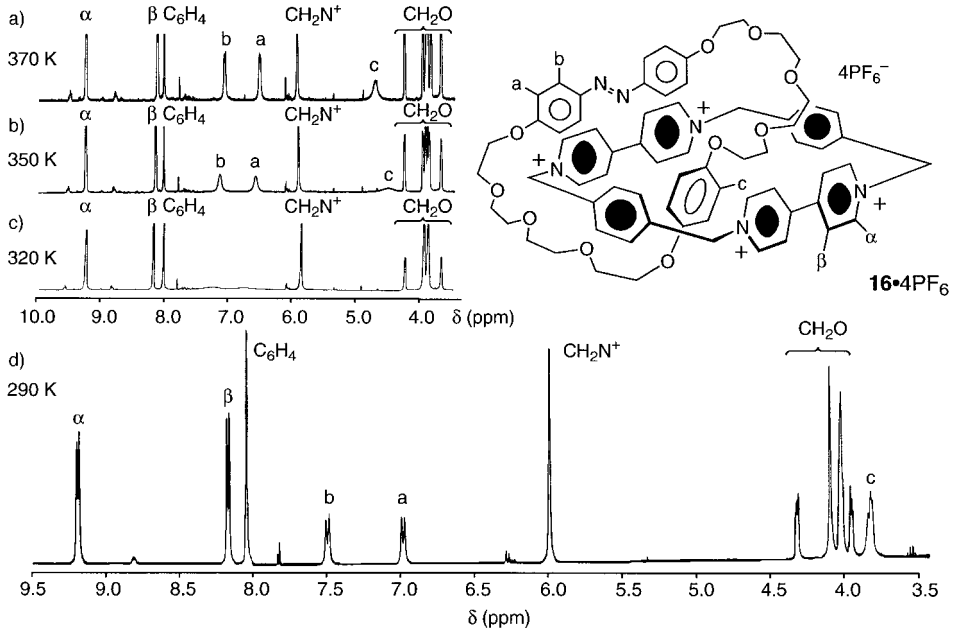

Figure 3. Partial ^{1}H NMR spectra of the [2]catenane **16**·4PF_6 recorded in $(CD_3)_2SO$ at a) 370, b) 350, and c) 320 K, and d) in $(CD_3)_2CO$ at 290 K.

Comparison of the ^{1}H NMR spectrum of the macrocyclic polyether **13** with that of the [2]catenane **17**·4PF_6 (Figure 4a)—both recorded in $(CD_3)_2SO$ at 380 K—shows upfield shifts for the 1,5-dioxynaphthalene protons. In particular, the protons in positions 4 and 8 on the 1,5-dioxynaphthalene ring undergo a shift of $\Delta\delta = -5.25$ ppm and resonate at $\delta = 2.50$ in the ^{1}H NMR spectrum of **17**·4PF_6. By contrast, the 4,4′-azobiphenoxy protons are only slightly affected ($\Delta\delta \cong -0.25$ ppm) suggesting that, under these conditions, the 1,5-dioxynaphthalene ring is located preferentially inside the cavity of the tetracationic cyclophane component. The protons in the α and β positions, with respect to the nitrogen atoms, on the bipyridinium units give rise to sharp and well-resolved signals in the ^{1}H NMR spectrum of **17**·4PF_6, recorded in $(CD_3)_2SO$ at 380 K, suggesting that the inside and alongside bipyridinium units are in fast exchange on the ^{1}H NMR timescale. On cooling a $(CD_3)_2CO$

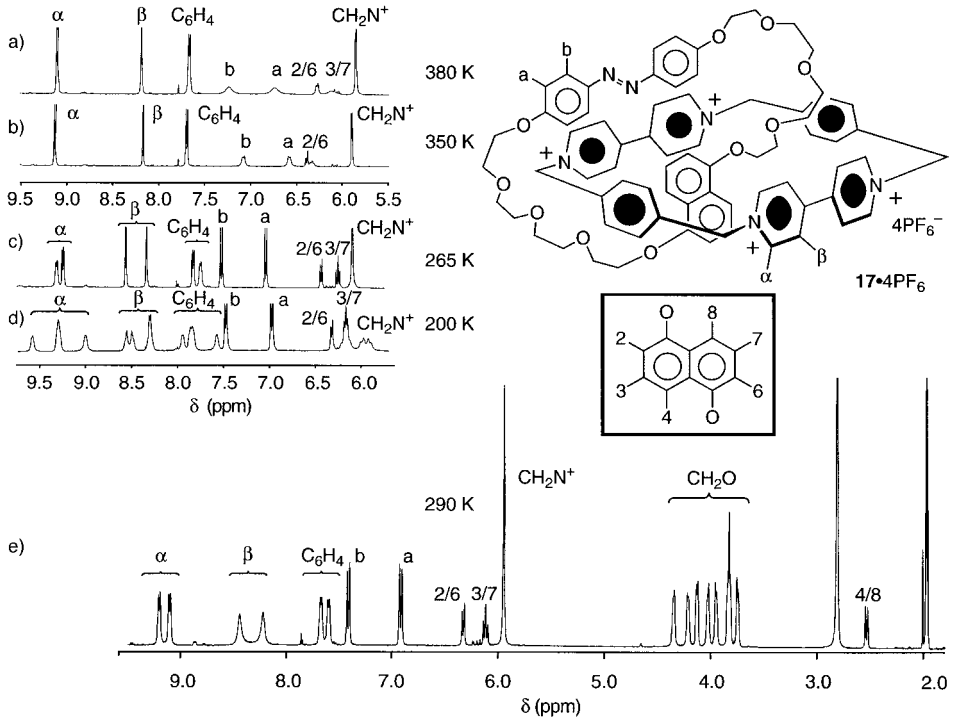

Figure 4. Partial ^{1}H NMR spectra of the [2]catenane **17**·4PF_6 recorded in $(CD_3)_2SO$ at a) 380 and b) 350, and in $(CD_3)_2CO$ at c) 265, d) 200, and e) 290 K.

0947-6539/99/0503-0864 $ 17.50+.50/0 *Chem. Eur. J.* **1999**, *5*, No. 3

solution of **17**·4PF$_6$ down, the resonances of the 1,5-dioxynaphthalene and 4,4′-azobiphenoxy protons become (Figure 4c and 4e) sharp in the ^{1}H NMR spectrum, suggesting that the circumrotation of the macrocyclic polyether through the cavity of the tetracationic cyclophane is now slow on the ^{1}H NMR timescale, and that the 1,5-dioxynaphthalene recognition site is located exclusively inside. As a result of the local C_{2h} symmetry of the 1,5-dioxynaphthalene unit, the protons in the α and β positions, with respect to the nitrogen atoms, on the bipyridinium units now give rise (Figure 4c and 4e) to two sets of signals in each case. On cooling a $(CD_3)_2CO$ solution of **17**·4PF$_6$ down to 200 K, the circumrotation of the tetracationic cyclophane through the cavity of the macrocyclic polyether also becomes slow on the ^{1}H NMR timescale, and all protons of the tetracationic cyclophane component give rise (Figure 4d) to three sets of signals.

The ^{1}H NMR spectrum of the [2]catenane **23**·4PF$_6$ in $(CD_3)_2CO$ at 323 K shows (Figure 5a) broad resonances for the 4,4′-azobiphenoxy protons. On cooling the solution down to 253 K, the 4,4′-azobiphenoxy protons give rise (Figure 5d) to four sets of signals in the ^{1}H NMR spectrum. Similarly, four sets of signals, centered on $\delta = 6.75$, 6.45, 4.25, and 3.45, respectively, are also observed for the protons attached to the two 1,4-dioxybenzene rings. These observations suggest that the macrocyclic polyether resides preferentially around one of the two 1,4-dioxybenzene rings, while the 4,4-azobiphenoxy unit and the other 1,4-dioxybenzene ring are located alongside. By contrast, the protons in the α and β positions, with respect to the nitrogen atoms, on the bipyridinium units give rise to only one resonance in each case, indicating that the circumrotation of the tetracationic cyclophane through the macrocyclic polyether component is fast on the ^{1}H NMR timescale at 253 K.

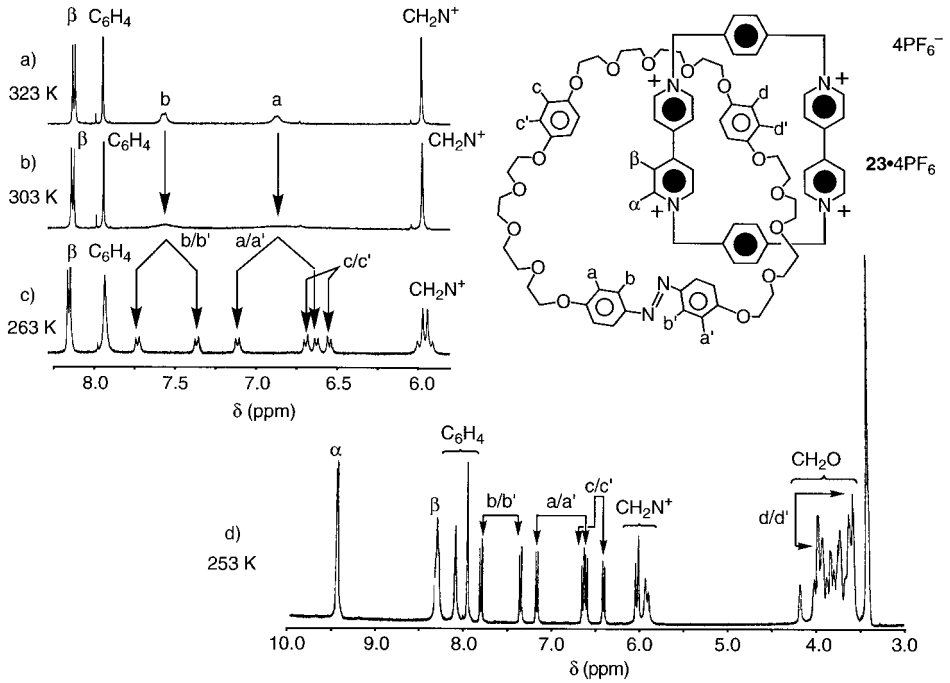

Figure 5. Partial ^{1}H NMR spectra of the [2]catenane **23**·4PF$_6$ recorded in $(CD_3)_2CO$ at a) 323, b) 303, c) 263, and d) 253 K.

The ^{1}H NMR spectra of CD_3CN solutions of the azobenzene-containing [2]catenanes **16**·4PF$_6$ and **17**·4PF$_6$, recorded after the irradiation ($\lambda = 360$ nm) of the solutions for 1 h at 298 K, did not reveal any significant changes. In both cases, the resonances characteristic of the *cis* isomer of the 4,4′-azobiphenoxy unit were not detected. However, comparison of the ^{1}H NMR spectra of a CD_3CN solution of the [2]catenane **23**·4PF$_6$, recorded before and after the irradiation ($\lambda = 360$ nm) of the solution for 1 h at 298 K, revealed the appearance of new resonances corresponding to an isomeric [2]catenane incorporating the *cis* form of the 4,4′-azobiphenoxy unit.

The ^{1}H NMR spectrum of the [2]rotaxane **30**·4PF$_6$ in CD_3CN at 245 K displays four sets of signals for the 4,4′-azobiphenoxy protons. On warming the solution up, the dynamic process, involving the shuttling of the tetracationic cyclophane along the linear portion of the dumbbell-shaped component, becomes fast on the ^{1}H NMR timescale, and the resonances of the 4,4′-azobiphenoxy protons coalesce into two sets of signals only.[9] Furthermore, a ^{1}H NMR spectrum of the same compound, recorded in $(CD_3)_2CO$ at 245 K, shows a singlet, centered on $\delta = 6.82$ that corresponds to the four protons of one of the two 1,4-dioxybenzene rings. The other 1,4-dioxybenzene ring is located exclusively inside the cavity of the tetracationic cyclophane component and its four protons presumably resonate at very much higher fields (we have not been able to locate the signal). The ^{1}H NMR spectrum of the [2]rotaxane in CD_3CN at 245 K, recorded after irradiation ($\lambda = 360$ nm) of the solution for 1 h at 298 K, revealed the appearance of new resonances corresponding to an isomeric [2]rotaxane incorporating the *cis* form of the 4,4′-azobiphenoxy unit.

X-ray crystallography: The X-ray structural analysis of the 1:1 complex formed between **1**·4PF$_6$ and **8** reveals (Figure 6) a disordered pseudorotaxane superstructure. The central thread unit adopts two C_i-related slipped positions with respect to the center of the tetracationic cyclophane, which is positioned about a crystallographic inversion center. The N=N bond is significantly displaced with respect to the centroid of the tetracationic cyclophane, with a mean interplanar separation of 3.5 Å between the N=N bond and the bipyridinium units. The [O···O] axis of the 4,4′-azobiphenoxy unit is inclined steeply (85°) with respect to the mean plane of the tetracationic cyclophane, thereby preventing any [C–H···π] interactions between the 4,4′-azobiphenoxy hydrogen atoms and the *p*-xylyl rings of the tetracationic cyclophane (the shortest

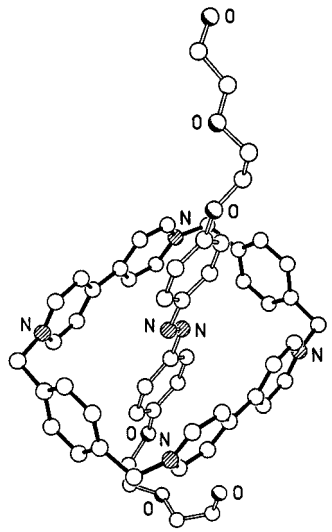

Figure 6. Ball-and-stick representation of the geometry adopted by the complex formed between $\mathbf{1}^{4+}$ and **8** in the solid state.

[H···π] distance is >3.3 Å). Because of the disorder, the position of the terminal hydroxyl hydrogen atoms could not be determined. However, there are no short inter- and/or intra-complex contacts indicative of hydrogen bonds being formed to these centers. It is interesting to note that the terminal hydroxyl group of one of the polyether chains is folded over and directed toward two adjacent hydrogen atoms in the β positions, with respect to the nitrogen atoms, on one of the bipyridinium units, but the shortest [H···O] distance is 3.31 Å and, thus precludes any [C–H···O] hydrogen bonding. Inspection of the packing of the 1:1 complexes did not reveal any π–π stacking or polypseudorotaxane formation.

The X-ray structural analysis of the macrocyclic polyether **13** reveals (Figure 7) that the 1,5-dioxynaphthalene ring is oriented almost orthogonally (86°) to the plane of one of the

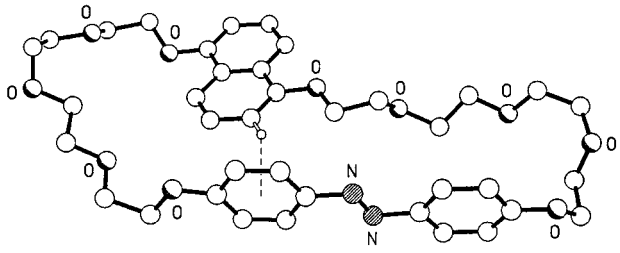

Figure 7. Ball-and-stick representation of the geometry adopted by the macrocyclic polyether **13** in the solid state.

phenoxy rings of the 4,4′-azobiphenoxy unit. This conformation is stabilized by a transannular [C–H···π] interaction between the hydrogen atom in position 2 on the 1,5-dioxynaphthalene ring and the facing phenoxy ring of the 4,4′-azobiphenoxy unit (the [H···π] distance is 2.72 Å and the [C–H···π] angle is 158°). There is evidence for a second, but much weaker, [C–H···π] interaction, between the other phenoxy ring of the 4,4′-azobiphenoxy unit and one of the methylene hydrogen atoms of the directly opposite chain (the [H···π] distance is 3.03 Å). The 4,4′-azobiphenoxy unit is nearly planar, the only deviation being a small torsional twist (ca. 5°) about one of the C–N bonds. Despite this near optimal geometry for conjugation, the two C–N bond lengths (1.462(3) and 1.464(3) Å) are typical of single C–N bonds, while the N=N] bond length (1.214(3) Å) is indicative of a strong double-bond character. The packing of the molecules does not reveal any significant intermolecular π–π, [C–H···π], and/or [C–H···O] interactions.

The X-ray structural analysis of the [2]catenane $\mathbf{17}\cdot 4PF_6$ shows (Figure 8) that the 1,5-dioxynaphthalene ring of the macrocyclic polyether is located inside the cavity of the

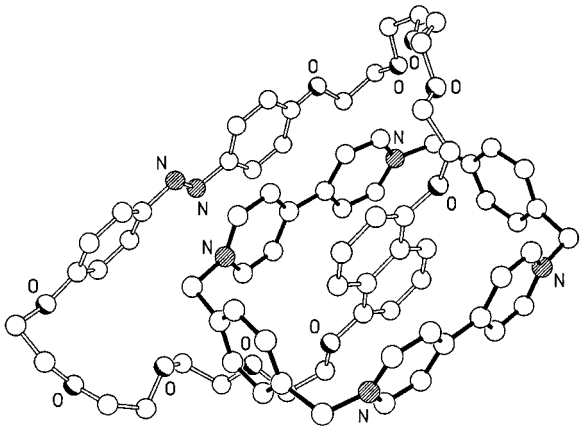

Figure 8. Ball-and-stick representation of the geometry adopted by the [2]catenane $\mathbf{17}^{4+}$ in the solid state.

tetracationic cyclophane, while the 4,4′-azobiphenoxy unit is positioned alongside. The mean interplanar separations between the 1,5-dioxynaphthalene ring and the inside and alongside bipyridinium units are 3.41 and 3.37 Å, respectively. The [O···O] vector of the 1,5-dioxynaphthalene unit is inclined by 50° with respect to the mean plane of the tetracationic cyclophane. The 4,4′-azobiphenoxy unit is offset with respect to the inside bipyridinium unit such that only one of the its phenoxy rings is involved in π–π stacking interactions (mean interplanar separation 3.38 Å). The 4,4′-azobiphenoxy unit has an approximate planar geometry with a small torsional twist (12°) about the C–N bond of the noninteracting end of this unit. The N=N bond is positioned almost centrally over one of the pyridinium rings, and the vector linking the center of the pyridinium ring and the center of the N=N bond is inclined by 82° to the N=N bond (the centroid–centroid separation is 3.47 Å). The [2]catenane is stabilized by the usual combination of [C–H···O], π–π, and [C–H···π] interactions. The [C–H···O] interactions involve the hydrogen atoms at the α positions with respect to the nitrogen atoms on the inside bipyridinium unit. In one case, these interactions are to the central oxygen atom in one of the polyether linkages (the [C···O] and [H···O] distances are 3.26, 2.34 Å, respectively, and the [C–H···O] angle is 153°) and, in the other, they are to the second oxygen atom away from the 1,5-dioxynaphthalene ring system in the other linkage (the [C···O] and [H···O] distances are 3.16 and 2.31 Å, respectively, and the [C–H···O] angle is 147°). There is another hydrogen bond interaction between one of the corner methylene hydrogen atoms of the tetracationic cyclo-

0947-6539/99/0503-0866 $ 17.50+.50/0 *Chem. Eur. J.* **1999**, *5*, No. 3

phane and the fourth oxygen atom away from the 1,5-dioxynaphthalene unit in one of the polyether linkages (the [C···O] and [H···O] distances are 3.06, 2.36 Å, respectively, and the [C–H···O] angle is 129). The [C–H···π] interaction between the inside 1,5-dioxynaphthalene ring and the *p*-xylyl rings of the tetracationic cyclophane have [H···π] distances of 2.52 and 2.59 Å and [C–H···π] angles of 157° and 149°, respectively. Inspection of the packing of the [2]catenane reveals (Figure 9) the formation of conventional polar stacks

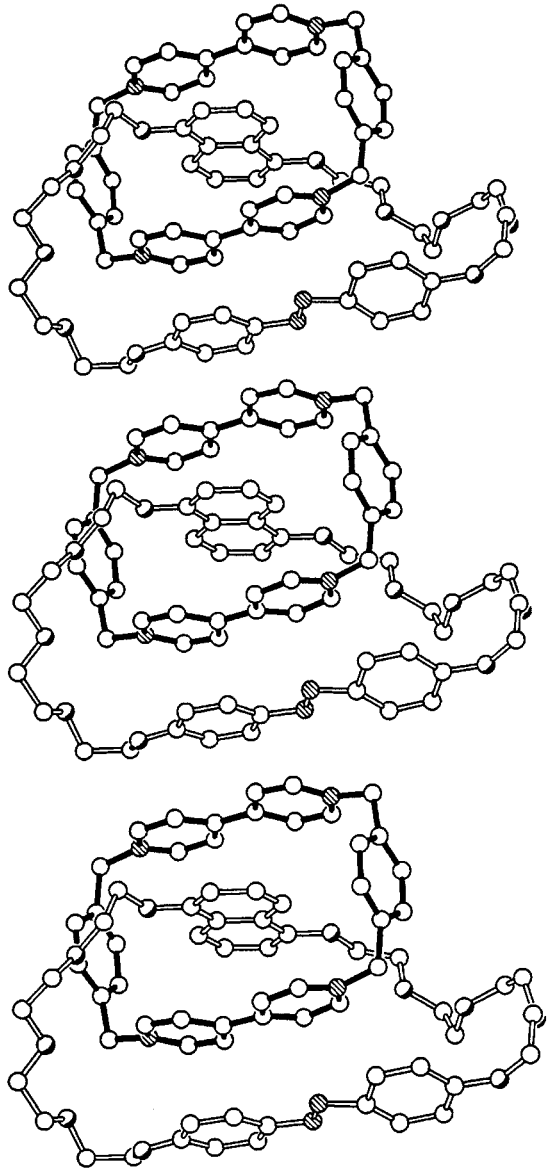

Figure 9. One of the donor–acceptor stacks formed by adjacent [2]catenanes $\mathbf{17}^{4+}$ in the crystal.

and produced by a lattice translation in the crystallographic *b* direction. The mean interplanar separation between one of the phenoxy rings of the alongside 4,4′-azobiphenoxy unit and the alongside bipyridinium unit is 3.34 Å. Adjacent polar stacks are offset, and the parallelly-aligned *p*-xylyl rings in adjacent stacks are separated by a distance that is too large for any π–π-stacking interaction. The included benzene solvent molecules sustain edge-to-face interactions (Figure 10) with

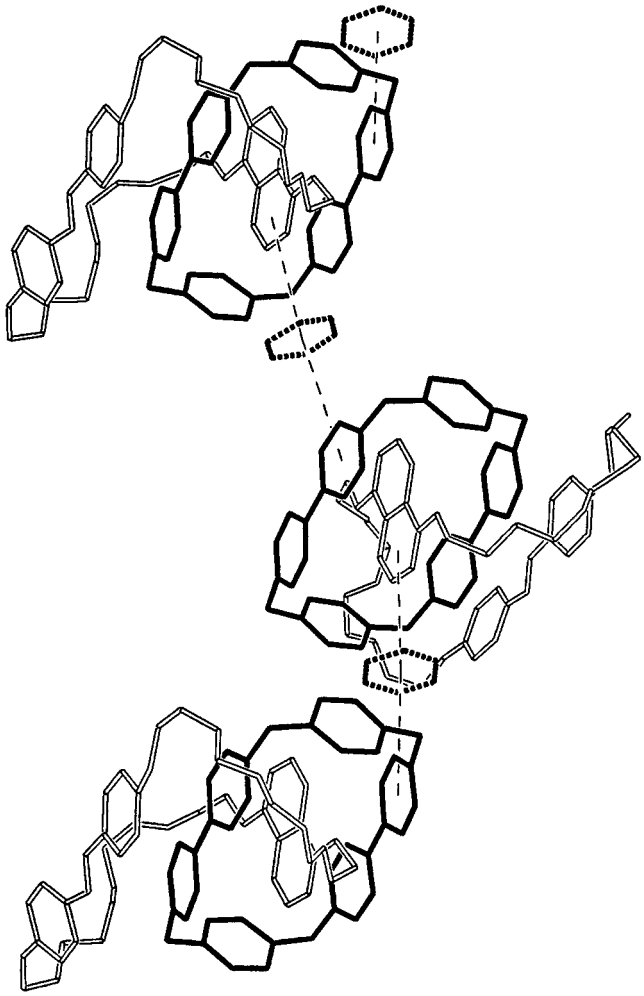

Figure 10. The edge-to-face interactions sustained by the included benzene solvent molecules and the [2]catenanes $\mathbf{17}^{4+}$ in the crystal.

one of the pyridinium rings of the alongside bipyridinium unit of one molecule and with the 1,5-dioxynaphthalene ring of another. The benzene ring is inclined by 80° to the pyridinium ring and by 81° to the 1,5-dioxynaphthalene ring. The centroid–centroid separation between the pyridinium ring and the benzene ring is 4.69 Å, while that to the center of the interacting ring of the 1,5-dioxynaphthalene unit is 4.64 Å. The two edge-to-face vectors subtend an angle of 176° at the center of the benzene ring. These combined interactions produce a continuous cascadelike arrangement of edge-to-face linked [2]catenanes and included benzene molecules.

Absorption spectra

Components: The absorption properties (MeCN solution, room temperature) of the photoisomerizable components of the catenanes and rotaxane are gathered in Table 1. The compound *trans*-4,4′-dimethoxyazobenzene, which has been chosen as a model for the *trans*-4,4′-azobiphenoxy unit present in the investigated species, shows the ππ* (λ_{max} = 355 nm) and nπ* (λ_{max} = 440 nm) bands characteristic of the *trans*-azobenzene unit (Table 1).[1a, 10] The ππ* band is 3500 cm^{-1} red-shifted compared with that of azobenzene.

Table 1. Absorption properties of the photoisomerizable molecular components.[a]

	trans Isomer		*cis* Isomer	
	λ_{max} [nm]	ε [$M^{-1}cm^{-1}$]	λ_{max} [nm]	ε [$M^{-1}cm^{-1}$]
4,4′-Dimethoxyazobenzene	355	28300	308	9200
	440[b]	1700	445	2700
12	299	6400	300	9800
	358	27000	445	2500
	440[b]	1700		
13	296	14400	297	17300
	358	28000	445	2700
	440[b]	1800		
22	291	9200	293	11900
	357	26900	445	2600
	440[b]	1800		
29	287	13900	287	16100
	356	25000	445	2500
	440[b]	1800		

[a] MeCN solution, room temperature. [b] Shoulder.

This observation is not surprising since substitution on the phenyl rings influences the position of the ππ* band, but not that of the nπ* band.[1a, 10] The nπ* absorption feature appears as a shoulder on the lower energy side of the more intense ππ* band. The absorption properties of the 1,4-dioxybenzene and 1,5-dioxynaphthalene units have been described in previous papers.[11] The absorption spectrum of the acyclic polyether **8** is identical to that of the model compound. The absorption spectra of the macrocyclic polyethers **12**, **13**, and **22**, and of the acyclic polyether **29** are approximately equal to the sum of the spectra of the *trans*-4,4′-azobiphenoxy group and of the other chromophoric units present in the compound (one 1,4-dioxybenzene in **12**, one 1,5-dioxynaphthalene in **13**, two 1,4-dioxybenzene in **22**, and two 1,4-dioxybenzene and two triphenyl(phenyloxy)methane in **29**).

Cis-4,4′-dimethoxyazobenzene (obtained photochemically from the *trans* form, see Experimental Section) shows (Table 1) the ππ* ($\lambda_{max} = 310$ nm) and nπ* ($\lambda_{max} = 445$ nm) bands characteristic of the *cis*-azobenzene unit.[1a, 10] When the *trans*-4,4′-azobiphenoxy moiety of compounds **8**, **12**, **13**, **22**, and **29** is photochemically converted to the *cis* form, the absorption spectra of the compounds are again those expected on the basis of their chromophoric units.

Catenanes and the r*otaxane*: The absorption spectra of the catenanes $\mathbf{16}^{4+}$, $\mathbf{17}^{4+}$, and $\mathbf{23}^{4+}$, and the rotaxane $\mathbf{30}^{4+}$ show several very intense bands in the UV region that can be assigned to ππ* transitions characteristic of the bipyridinium units of $\mathbf{1}^{4+}$ (λ_{max} around 260 nm)[11] and of the *trans*-4,4′-azobiphenoxy unit (λ_{max} around 360 nm; see, e.g., Figure 11). The less intense ^{1}ππ* absorption bands of 1,4-dioxybenzene, 1,5-dioxynaphthalene, and triphenyl(phenyloxy)methane units—contained in $\mathbf{16}^{4+}$, $\mathbf{23}^{4+}$ and $\mathbf{30}^{4+}$, in $\mathbf{17}^{4+}$, and in $\mathbf{30}^{4+}$, respectively—lie in the 280–300 nm region and therefore are hidden by the very intense $\mathbf{1}^{4+}$ bands. The vibrational structure characteristic of the absorption band of the 1,5-dioxynaphthalene unit is lost (Figure 11) in the catenane $\mathbf{17}^{4+}$, as previously observed for related compounds.[11b] In the visible region, the spectra of the rotaxane and catenanes show the weak ^{1}nπ* band of the 4,4′-azobiphenoxy group, with a red-

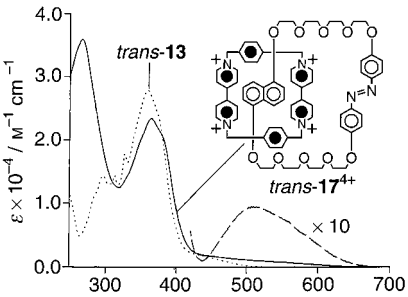

Figure 11. Absorption spectrum (MeCN, room temperature) of the [2]catenane *trans*-$\mathbf{17}^{4+}$ (full line), of its macrocyclic polyether component *trans*-**13** (dotted line), and their difference in the visible region (dashed line).

side tail that can be attributed to a charge-transfer (CT) interaction between the 1,4-dioxybenzene and 1,5-dioxynaphthalene units of the macrocyclic polyether and thread components and the bipyridinium units of the cyclophane $\mathbf{1}^{4+}$.[11] The maximum of the CT band, when the electron-donor unit interacting with $\mathbf{1}^{4+}$ is 1,4-dioxybenzene, is expected to be around 470–480 nm on the basis of results previously obtained[11a] for a related [2]rotaxane ($\lambda_{max} =$ 470 nm; $\varepsilon = 350\ M^{-1}cm^{-1}$) and [2]catenane ($\lambda_{max} =$ 478 nm; $\varepsilon = 700\ M^{-1}cm^{-1}$). Therefore, in *trans*-$\mathbf{16}^{4+}$, the CT band is partially hidden by the more intense ^{1}nπ* band of the 4,4′-azobiphenoxy unit, but it can be seen ($\lambda_{max} \approx 490$ nm; $\varepsilon \approx 500\ M^{-1}cm^{-1}$) by subtraction of the absorption spectrum of *trans*-**12** from that of *trans*-$\mathbf{16}^{4+}$. In the case of catenane $\mathbf{17}^{4+}$, in which the electron donor is the 1,5-dioxynaphthalene unit, the CT band is displaced toward lower energy, in agreement with the behavior found for a related [2]pseudorotaxane ($\lambda_{max} = 529$ nm; $\varepsilon = 1100\ M^{-1}cm^{-1}$)[12] and [2]catenane ($\lambda_{max} =$ 515 nm; $\varepsilon = 650\ M^{-1}cm^{-1}$).[11b] From the subtraction of the absorption spectrum of the macrocyclic polyether *trans*-**13** from that of the corresponding [2]catenane *trans*-$\mathbf{17}^{4+}$ in the visible region, the CT band is found (Figure 11) to have $\lambda_{max} \approx$ 510 nm and $\varepsilon \approx 1000\ M^{-1}cm^{-1}$.

The same kind of arithmetical operations on the spectra of the respective components gives bands with $\lambda_{max} \approx 480$ nm ($\varepsilon \approx 600\ M^{-1}cm^{-1}$) for the catenane $\mathbf{23}^{4+}$ and with $\lambda_{max} \approx$ 490 nm ($\varepsilon \approx 300\ M^{-1}cm^{-1}$) for the rotaxane $\mathbf{30}^{4+}$. Interestingly, there are no appreciable variations in the energies and intensities of such bands upon photoisomerization of the 4,4′-azobiphenoxy unit of $\mathbf{23}^{4+}$ and $\mathbf{30}^{4+}$. This observation suggests that the geometrical changes associated with the isomerization processes do not affect significantly the interactions between the dioxybenzene and bipyridinium units.

Although a charge-transfer interaction may also be expected to occur between the 4,4′-azobiphenoxy group and the bipyridinium units, no band attributable to this interaction can be observed, presumably because it is hidden by the much more intense absorption bands present in the UV region.

Fluorescence properties

Components: It has been established previously[11a] that $\mathbf{1}^{4+}$ is not emissive. *Trans*- and *cis*-4,4′-dimethoxyazobenzene do not show any luminescence either in MeCN solution at room

0947-6539/99/0503-0868 $ 17.50+.50/0 *Chem. Eur. J.* **1999**, *5*, No. 3

temperature or in butyronitrile rigid matrix at 77 K. This observation is in line with the behavior of nonrigid azobenzene-type molecules.[1a, 10]

The fluorescence of the 1,4-dioxybenzene and 1,5-dioxynaphthalene units[11] are strongly quenched, both at room temperature and at 77 K, when such units are incorporated into the macrocyclic polyethers **12**, **13**, and **22**, and also in the acyclic polyether **29**. This result can be accounted for by the presence of low-energy excited states on the 4,4′-azobiphenoxy unit that can quench, by energy transfer, the upper lying, potentially luminescent excited states of the other chromophoric groups. An energy-transfer-quenching mechanism is confirmed by the results of the photochemical experiments discussed later. In the macrocyclic polyethers **12** and **13**, the residual fluorescence of the 1,4-dioxybenzene and 1,5-dioxynaphthalene units at room temperature is at least 200 and 450 times weaker, respectively, than that of the 1,4-dimethoxybenzene and 1,5-dimethoxynaphthalene model compounds. For the thread **29**, the presence of strongly fluorescent 1,4-dioxybenzene-type impurities (confirmed by fluorescence lifetime measurements and TLC tests) did not allow a quantitative evaluation of the amount of energy-transfer quenching. Macrocyclic polyether **22** exhibits two emission bands at room temperature, with maxima at 325 nm (characteristic of dioxybenzene units) and 380 nm. Excitation spectra and luminescence lifetime measurements suggest the attribution of the 325 nm band to small amounts ($\leq 1.5\,\%$) of 1,4-dioxybenzene-type impurities, rather than to the residual emission of the dioxybenzene-type units of **22**. The 380 nm band ($\Phi = 6 \times 10^{-3}$; $\tau = 4.5$ ns) originates from an interaction between the two dioxybenzene moieities, a phenomenon which has been observed previously in a dendritic compound based on similar oxybenzene units.[13] The fluorescence of the dioxyarene units in compounds **12**, **13**, **22**, and **29** is also strongly quenched when the *trans*-4,4′-azobiphenoxy unit is converted photochemically into the *cis* form.

The 1,5-dioxynaphthalene unit shows a more intense fluorescence compared with that of the 1,4-dioxybenzene unit.[11b] This difference means that a careful study of the energy-transfer quenching processes in *trans*- and *cis*-**13** can be initiated. Although the process is very efficient for both isomers, it is more than three times faster for the *trans* ($k_{en} \geq 7 \times 10^{10}\ s^{-1}$) than for the *cis* form ($k_{en} \approx 2 \times 10^{10}\ s^{-1}$)[14] (Figure 12). Since CPK space-filling molecular models show that the two chromophoric units of **13**, which are connected by flexible polyether chains, can come in close contact, regardless of the isomeric form of the 4,4′-azobiphenoxy unit, the higher efficiency of the energy-transfer process in *trans*-**13** cannot be ascribed to structural factors. Therefore, it seems reasonable to attribute the different behavior to a larger overlap between the fluorescence band of the 1,5-dioxynaphthalene unit ($\lambda_{max} = 345$ nm) and the $\pi\pi^*$ absorption band of the *trans*-4,4′-azobiphenoxy group ($\lambda_{max} = 358$ nm). In compound **22**, the intensity of the emission band at 380 nm does not depend on the isomeric form of the 4,4′-azobiphenoxy unit. This observation is not surprising, since both isomers of this molecule are very flexible, at least as indicated by inspection of CPK space-filling molecular models.

Catenanes and the rotaxane: The catenanes and the rotaxane are not luminescent because of the presence of the low-energy, nonemitting CT levels. This matter has been discussed elsewhere in the case of related systems.[11, 12]

Photoisomerization

Components: The quantum yields of the *trans* → *cis* and *cis* → *trans* photoisomerization reactions (air-equilibrated MeCN solution, room temperature) are listed in Table 2. A comparison of the isomerization quantum yields of **12**, **13**, **22** and **29** with those of the 4,4′-dimethoxyazobenzene model compound indicate (Table 2) that neither the macrocyclic nor the acyclic structures hinder the photoisomerization of the azobiphenoxy unit.[15]

Table 2. Photoisomerization quantum yields at different irradiation wavelength of the *trans* and *cis* isomers of the [2]rotaxane, the [2]catenanes, and their components.[a]

	$\Phi_{t\rightarrow c}$			$\Phi_{c\rightarrow t}$	
	287 nm	365 nm	436 nm	287 nm	436 nm
4,4′-Dimethoxyazobenzene	–	0.35	0.36	0.40	0.52
12	0.38	0.34	0.29	0.43	0.53
13	0.35	0.32	0.29	0.33	0.46
22	0.40	0.40	0.36	0.40	0.51
29	0.33	0.32	0.13	0.31	0.54
$\mathbf{16}^{4+}$	[b]	0.007	[b]	[b,c]	[b]
$\mathbf{17}^{4+}$	[b]	0.006	[b]	[b,c]	[b]
$\mathbf{23}^{4+}$	[b]	0.076	[b]	[b,c]	[b]
$\mathbf{30}^{4+}$	[b]	0.17	[b]	[b]	0.34

[a] MeCN solution, room temperature. [b] Not performed because of difficulties related to overlapping bands. [c] It was not possible to obtain the *cis* isomer because of the low value of $\Phi_{t\rightarrow c}$.

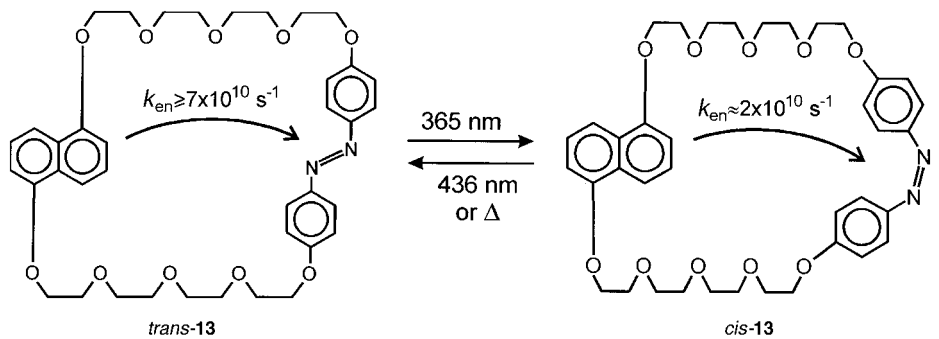

Figure 12. Schematic representation of the modulation of the energy transfer between the chromophoric units of the macrocyclic polyether **13** upon photoisomerization of its 4,4′-azobiphenoxy unit.

It is important to note that the quantum yield of *trans* → *cis* photoisomerization of **12**, **13**, **22**, and **29** does not change when irradiation is performed at 287 nm, a wavelength at which at least 50 % of the light is absorbed by the 1,4-dioxybenzene, 1,5-dioxynaphthalene, or 4-(tris(phenyl)methyl)phe-

nyloxy units. This observation is consistent with a very efficient energy-transfer process from the latter units to the *trans*-4,4′-azobiphenoxy group. Also, in the case for the *cis* → *trans* reaction, the photoisomerization quantum yield upon irradiation at 287 nm is close to that found for the 4,4′-dimethoxyazobenzene model compound. This observation suggests that the excitation energy is once again transferred from the $^1\pi\pi^*$ states of the 1,4-dioxybenzene or 1,5-dioxynaphthalene chromophores to the $^1\pi\pi^*$ state of the *cis*-4,4′-azobiphenoxy unit. However, for the compounds of the *cis*-family, the $\pi\pi^*$ band of the 4,4′-azobiphenoxy unit overlaps the $\pi\pi^*$ absorption bands of the other chromophoric groups. Therefore, it is not possible to measure the *cis* → *trans* photoisomerization quantum yield upon direct and exclusive excitation of the *cis*-4,4′-azobiphenoxy unit. Consequently, the contribution of the energy-transfer process to the *cis* → *trans* photoisomerization cannot be assessed quantitatively in the case of **12**, **13**, **22**, and **29**.

Pseudorotaxanes: We know that the *trans* form of the azobenzene-based threads is bound by $\mathbf{1}^{4+}$, whereas there is no evidence of association in the case of the *cis* isomer. We have studied the *trans* ⇌ *cis* photoisomerization of **8** alone, as well as in the presence of an excess of $\mathbf{1}^{4+}$ in air-equilibrated MeCN solution at room temperature. The concentrations of **8** and $\mathbf{1}^{4+}$ were 7.0×10^{-5} M and 2×10^{-3} M, respectively. We found that the quantum yields of the *trans* → *cis* photoreaction are 0.34 for **8** alone and 0.21 in the presence of $\mathbf{1}^{4+}$, whereas the corresponding quantum yields for the *cis* → *trans* photoisomerization are 0.52 and 0.42, respectively. Considering the large experimental error (±15%), we can conclude that the presence of $\mathbf{1}^{4+}$ decreases the quantum yield of the *trans* → *cis* photoisomerization in comparison with that of the *cis* → *trans* reaction. Since we have also found that, under the same experimental conditions, addition of 1,1′-dimethyl-4,4′-bipyridinium to a solution containing the thread **8** does not cause any effect, the influence of $\mathbf{1}^{4+}$ on the *trans* → *cis* photoisomerization of **8** can be attributed to the formation of a pseudorotaxane between *trans*-**8** and $\mathbf{1}^{4+}$, as indicated by NMR spectroscopic studies. On the basis of the association constant of 469 M^{-1} obtained from NMR measurements, about 50% of *trans*-**8** is threaded through $\mathbf{1}^{4+}$ under the conditions used by us. Since the exciting light is absorbed equally by complexed and uncomplexed *trans*-**8**, and the photoisomerization quantum yield for the unthreaded fraction is 0.34, we can estimate that the photoisomerization quantum yield of threaded *trans*-**8** is about 0.1. It is difficult to say whether such a decreased photoreactivity is a consequence of electronic or of steric effects.

Finally, we have found that the rate of the dark *cis* → *trans* isomerization is not influenced by the presence of $\mathbf{1}^{4+}$; an observation that is consistent with the lack of interaction between *cis*-**8** and $\mathbf{1}^{4+}$.

Catenanes and the rotaxane: When the acyclic polyether **29** and the macrocyclic polyethers **12**, **13**, and **22** are mechanically interlocked with the tetracationic cyclophane in the [2]rotaxane $\mathbf{30}^{4+}$ and in the [2]catenanes $\mathbf{16}^{4+}$, $\mathbf{17}^{4+}$, and $\mathbf{23}^{4+}$, their photoreactivity is considerably smaller (Table 2). In particular, for the [2]catenanes $\mathbf{16}^{4+}$ and $\mathbf{17}^{4+}$, the *trans* → *cis* photoisomerization quantum yields ($\lambda_{irr} = 365$ nm) are about 48 and 55 times smaller, respectively, than for the corresponding macrocyclic polyethers. For catenane $\mathbf{23}^{4+}$ (based on the larger macrocyclic polyether **22**) and the [2]rotaxane $\mathbf{30}^{4+}$ (containing the long acyclic polyether **29**), the quantum yield of the *trans* → *cis* isomerization is only 5 and 1.8 times smaller than those of **22** and **29**, respectively. Figure 13 shows the absorption changes obtained by irradiation of the rotaxane at 365 nm. The results obtained are consistent with the molecular structure and photophysical properties of the rotaxane. The decrease of the *trans* → *cis* photoisomerization yields of the 4,4′-azobiphenoxy unit in the rotaxane and catenane structures can be accounted for by the presence of low-lying charge-transfer excited states, which offer a fast radiationless decay to the azobiphenoxy excited states responsible for the photoisomerization. Such a decay process must be very fast to compete with the photoisomerization, which is known to occur in the sub-nanosecond timescale.[1a] In the smaller catenanes, radiationless deactivation is likely to be more effective because the 4,4′-azobiphenoxy group is obliged to remain close to the tetracationic cyclophane. In principle, another reason for the much lower photoreactivity of the smaller catenanes could be the fact that the photoisomerization of the azobiphenoxy moiety is hampered by steric reasons. However, inspection of CPK space-filling molecular models does not reveal any significant steric hindrance.

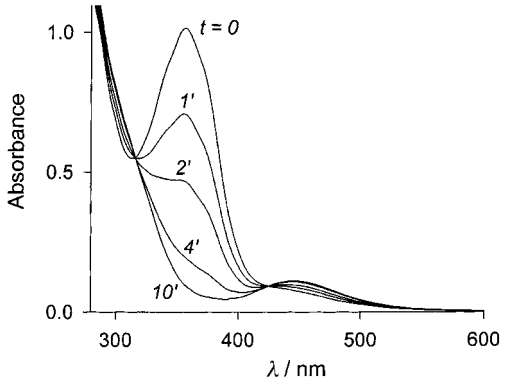

Figure 13. Spectral changes obtained upon irradiation of the [2]rotaxane $\mathbf{30}^{4+}$ at 365 nm in MeCN solution at room temperature.

In the larger [2]catenane $\mathbf{23}^{4+}$, the tetracationic cyclophane, which circumrotates around the macrocyclic polyether **22** on the ms timescale, prefers to interact with the two 1,4-dioxybenzene units rather than with the 4,4-azobiphenoxy group (see subsection on ^{1}H NMR spectroscopy). As a result, there are long-living co-conformations (compared with the time required for the isomerization) in which the 4,4′-azobiphenoxy moiety, being far from the charge-transfer region of the molecule, is free to isomerize. A similar explanation can be invoked in the case of the [2]rotaxane $\mathbf{30}^{4+}$, in which the tetracationic cyclophane can shuttle back and forth between the stations of the dumbbell-shaped component, probably spending most of the time around one of the two 1,4-dioxybenzene units.

0947-6539/99/0503-0870 $ 17.50+.50/0 *Chem. Eur. J.* **1999**, *5*, No. 3

Conclusion

Decomplexation/complexation cycles of two supramolecular complexes of a pseudorotaxane type, incorporating a 4,4′-azobiphenoxy unit in their thread-like components with respect to the cyclobis(paraquat-*p*-phenylene) tetracation, have been achieved by the reversible photoisomerization of the 4,4′-azobiphenoxy unit from *trans* to *cis*, and then back from *cis* to *trans* forms, respectively. By contrast, electronic effects and/or geometrical constraints render this isomerization much more difficult in two related [2]catenanes, locking the 4,4′-azobiphenoxy unit into the *trans* form only. However, by introducing greater flexibility into the azobenzene-containing components of one particular [2]catenane and [2]rotaxane, in each case, an efficient reversible photoisomerization of the 4,4′-azobiphenoxy unit can be observed. These photoactive supramolecular and molecular species can be regarded as prototypes for more complex systems able to perform logical operations at the molecular level.

Experimental Section

General methods: Solvents were purchased from Aldrich and purified according to literature procedures.[16] Reagents were purchased from Aldrich except for **1**·4PF_6,[17] **3**,[18] **6**,[19] **10**,[11a] **11**,[20] **14**·2PF_6,[11a] **18**,[18] **21**,[11a], **24**,[11a] and 4,4′-dimethoxyazobenzene,[21] which were synthesised according to literature procedures. Thin-layer chromatography (TLC) was carried out with aluminium sheets, precoated with silica gel 60F (Merck 5554) or aluminium oxide 60F_{254} neutral (Merck 5550). The plates were inspected by UV light prior to development with iodine vapor or by treatment with ceric ammonium molybdate reagent and subsequent heating. Melting points were determined on an Electrothermal 9200 apparatus and are uncorrected. Elemental analyses were performed by the University of London Microanalytical Laboratories. Electron impact mass spectra (EIMS) were recorded on a Kratos Profile spectrometer. Liquid secondary ion mass spectra (LSIMS) were recorded on a VG Zabspec triple focussing mass spectrometer. High resolution mass spectra (LSIMS) were obtained the VG Zabspec operating at a resolution of 6000 and with voltage scanning with CsI as a reference. ^{1}H NMR Spectra were recorded on Bruker AC300 (300 MHz), AMX400 (400 MHz), and/or DRX500 (500 MHz) spectrometers. ^{13}C NMR Spectra were recorded on a Bruker AC300 (75.5 MHz) with the JMOD pulse sequence. All chemical shifts are quoted in ppm on the δ scale with TMS or the solvent as an the internal standard. The coupling constants are expressed in Hz. Irradiation of samples for the ^{1}H NMR spectroscopic studies was carried out for 1 h at 298 K with a medium-pressure mercury vapor lamp fitted with a filter (UG5 for $\lambda = 360$ nm and UG1 for $\lambda = 440$ nm). High performance liquid chromatography (HPLC) was performed on Phenomenex Prodigy (spherical silicon) or Phenomenex IB-Sil C-18 columns (250 × 10 mm), eluted over Gilson 305 and 306 HPLC pumps. The pumps were controlled by external Gilson 715 software running on a 486 PC, and a Dynamax UV-1 ultraviolet detector was used.

2-{2-[2-(4-*tert*-Butylphenoxy)ethoxy]ethoxy}ethanol (**4**): A solution of **2** (21.20 g, 159 mmol) and **3** (43.00 g, 142 mmol) in dry MeCN (500 mL), containing K_2CO_3 (40.00 g, 280 mmol), was heated under reflux and an atmosphere of N_2 for 4 d. After cooling down to room temperature, the solvent was removed under vacuum. The residue was dissolved in CH_2Cl_2 (250 mL), washed with brine (3 × 250 mL), and dried ($MgSO_4$). The solution was concentrated under reduced pressure, and the residue was purified by column chromatography (SiO_2, CH_2Cl_2/MeOH, 100:2) to afford **4** (31.9 g, 79%) as a colorless oil. EIMS: *m/z* (%): 282 (85) $[M]^+$; ^{1}H NMR ($CDCl_3$): $\delta = 7.43-7.26$ (m, 2H), 6.86–6.78 (m, 2H), 4.20–4.05 (m, 2H), 3.92–3.80 (m, 2H), 3.72–3.60 (m, 6H), 3.58–3.51 (m, 2H), 1.25 (s, 9H); ^{13}C NMR ($CDCl_3$): $\delta = 126.2$, 114.1, 72.5, 70.8, 70.4, 69.8, 67.4, 61.8, 31.5, 22.9; $C_{16}H_{26}O_4$ (282.6): calcd C 68.06, H 9.28; found C 68.08, H 9.23.

2-{2-[2-(4-*tert*-Butylphenoxy)ethoxy]ethoxy}ethanoltosylate (**5**): A solution of *p*-toluenesulfonyl chloride (16.50 g, 89 mmol) in THF (100 mL) was added dropwise over 1 h to a solution of **5** (25.00 g, 89 mmol) and NaOH (4.60 g, 115 mmol) in THF (80 mL) and H_2O (50 mL) mantained at −5 °C. The mixture was stirred for further 3 h at −5 °C, poured into ice/H_2O (300 mL), and washed with CH_2Cl_2 (3 × 150 mL). The organic layer was dried ($MgSO_4$) and concentrated under reduced pressure. The resulting oil was purified by column chromatography (SiO_2, CH_2Cl_2/MeOH, 100:1) to afford **5** (36.2 g, 94%) as a colorless oil. (LSIMS): *m/z*: 434 $[M]^+$; ^{1}H NMR ($CDCl_3$): $\delta = 7.85-7.75$ (m, 2H), 7.40–7.15 (m, 4H), 6.85–6.70 (m, 2H), 4.25–4.15 (m, 2H), 4.15–4.05 (m, 2H), 3.85–3.80 (m, 2H), 3.70–3.50 (m, 6H), 2.43 (s, 3H), 1.25 (s, 9H); ^{13}C NMR ($CDCl_3$): $\delta = 156.4$, 144.8, 143.6, 133.0, 129.8, 128.0, 126.2, 114.0, 70.8, 69.8, 69.3, 68.8, 67.4, 31.6, 21.7; $C_{23}H_{32}O_6S$ (432.8): calcd C 63.28, H 7.39; found C 63.38, H 7.42.

4,4′-Bis[2-(2-hydroxyethoxy)ethoxy]azobenzene (**8**): A solution of **6** (3.91 g, 18 mmol) and **7** (4.53 g, 37 mmol) in dry MeCN (200 mL), containing K_2CO_3 (26.0 g, 185 mmol), was heated under reflux and an atmosphere of N_2 for 4 d. After cooling down to room temperature, the solvent was removed under vacuum and the residue was dissolved in CH_2Cl_2 (250 mL), washed with brine (3 × 250 mL), and dried ($MgSO_4$). The solution was concentrated under reduced pressure, and the solid residue was crystallized from MeCN to afford a yellow powder (3.93 g). A small portion of the powder (100 mg) was purified by HPLC, employing a Phenomenex Prodigy (spherical silicon) column (250 × 10 mm) and eluting at 2.5 mL min^{-1} with 5% MeOH in CH_2Cl_2, to afford **8** (90 mg) as a yellow solid. M.p. 67 °C; LSIMS: *m/z*: 391 $[M]^+$; ^{1}H NMR ($CDCl_3$): $\delta = 7.94-7.80$ (m, 4H), 7.08–6.95 (m, 4H), 4.29–4.25 (m, 4H), 3.95–3.85 (m, 4H), 3.82–3.60 (m, 4H), 3.60–3.50 (m, 4H), 2.24 (s, 2H); ^{13}C NMR ($CDCl_3$): $\delta =$ 160.7, 147.2, 124.4, 114.8,72.7, 69.6, 67.7, 61.8; $C_{20}H_{26}N_2O_6$ (390.4): calcd C 61.54, H 6.67, N 7.18; found C 61.43, H 6.69, N 7.23. Single crystals of the complex [**1**:**8**]·4PF_6 suitable for X-ray crystallographic analysis were grown by vapor diffusion of *i*Pr_2O into an equimolar MeCN solution of **1**·4PF_6 and **8**.

4,4′-Bis{2-[2-[2-(4-*tert*-butylphenoxy)ethoxy]ethoxy}ethoxy}azobenzene (**9**): A solution of **6** (2.45 g, 11 mmol) and **5** (10.00 g, 23 mmol) in dry MeCN (250 mL), containing K_2CO_3 (16.00 g, 115 mmol), was heated under reflux and an atmosphere of N_2 for 4 d. After cooling down to room temperature, the solvent was removed under vacuum, and the residue was dissolved in CH_2Cl_2 (250 mL), washed with brine (3 × 250 mL), and dried ($MgSO_4$). The solution was concentrated under reduced pressure to afford a yellow powder (5.84 g). A small portion of the powder (100 mg) was purified by HPLC, employing a Phenomenex IB-SIL (Base-deactivated ODS) column (250 × 10 mm) and eluting at 2.5 mL min^{-1} with MeCN, to afford **9** (85 mg) as a yellow solid. M.p. 88 °C; LSIMS: *m/z*: 742 $[M]^+$; HRMS (LSIMS): calcd for $[M]^+$ ($C_{44}H_{59}N_2O_8$) 743.4271, found 743.4267; ^{1}H NMR (CD_3CN): $\delta = 7.86-7.80$ (m, 4H), 7.31–7.20 (m, 4H), 7.10–7.01 (m, 4H), 6.81–6.71 (m, 4H), 4.25–4.15 (m, 4H), 4.10–4.00 (m, 4H), 3.85–3.73 (m, 4H), 3.70–3.65 (m, 4H), 3.63 (s, 8H), 1.25 (s, 18H); ^{13}C NMR (CD_3CN): $\delta = 162.1$, 157.7, 147.9, 144.4, 127.3, 125.2, 118.2, 115.9, 115.0, 71.5, 71.4, 70.5, 70.3, 68.9, 68.4, 34.7, 31.8.

4,4′-Azophenyl-*p*-phenylene-40-crown-10 (**12**): A solution of **10** (15.57 g, 19 mmol) in dry DMF (100 mL) was added dropwise over 3 h to a solution of **6** (4.06 g, 19 mmol) in dry DMF (450 mL), containing Cs_2CO_3 (136.30 g, 419 mmol) and CsOTs (13.60 g), maintained at 80 °C under an atmosphere of N_2. The mixture was stirred for a further 3 d at 80 °C and, after cooling down to room temperature, the solvent was removed under vacuum. The residue was dissolved in CH_2Cl_2 (150 mL), washed with H_2O (4 × 150 mL) and dried ($CaCl_2$). Removal of the solvent under reduced pressure gave an oil, which was purified by column chromatography (SiO_2, Et_2O/$CHCl_3$/MeOH, 68:30:2) to yield **12** (1.92 g, 15%) after crystallization from $CHCl_3$/hexane (9:1). M.p. 85–87 °C; LSIMS: *m/z*: 641 $[M+H]^+$; ^{1}H NMR ($CDCl_3$): $\delta = 7.92-7.80$ (m, 4H), 7.08–6.95 (m, 4H), 6.52 (s, 4H), 4.32–3.50 (m, 32H); ^{13}C NMR ($CDCl_3$): $\delta = 160.9$, 152.9, 147.1, 124.4, 115.2, 114.6, 71.0, 70.9, 70.8, 70.5, 69.9, 69.7, 68.1; $C_{34}H_{44}O_{10}N_2$ (640.2): calcd C 63.75, H 6.88, N 4.38; found C 63.66, H 6.87, N 4.55.

4,4′-Azophenyl-1,5-naphtho-42-crown-10 (**13**): A solution of **11** (15.12 g, 19 mmol) in dry DMF (100 mL) was added dropwise over 3 h to a solution of **6** (4.06 g, 19 mmol) in dry DMF (450 mL), containing Cs_2CO_3 (136.30 g, 419 mmol) and CsOTs (13.60 g), maintained at 80 °C under an atmosphere of N_2. The mixture was stirred at 80 °C for a further 3 d and, after cooling down to room temperature, the solvent was removed under vacuum. The

residue was dissolved in CH_2Cl_2 (150 mL), washed with H_2O (4 × 150 mL), and dried ($CaCl_2$). Removal of the solvent under reduced pressure gave an oil, which was purified by column chromatography (SiO_2, $Et_2O/CHCl_3$/MeOH, 68:30:2) to yield **13** (3.28 g, 21%) after crystallization from $CHCl_3$/hexane (9:1). M.p. 85–87 °C; LSIMS: *m/z*: 690 $[M]^+$; ^{1}H NMR ($CDCl_3$): $\delta = 7.78–7.73$ (m, 6H), 7.19–7.09 (m, 2H), 6.98–6.94 (m, 4H), 6.51 (d, 2H), 4.22 (m, 4H), 4.09 (m, 4H), 3.90 (m, 8H), 3.76 (m, 16H); ^{13}C NMR ($CDCl_3$): $\delta = 160.8, 154.2, 147.1, 126.7, 125.0, 124.2, 115.1, 105.5, 71.1, 70.8, 69.9, 68.0, 67.7$; $C_{38}H_{46}O_{10}N_2$ (690.0): calcd C 66.06, H 6.72, N 4.06; found C 66.01, H 6.75, N 3.97. Single crystals suitable for X-ray crystallographic analysis were grown by vapor diffusion of *i*Pr_2O into a MeCN solution of **13**.

[2]Catenane 16·4PF$_6$: A solution of **12** (230 mg, 0.36 mmol), **14·2PF$_6$** (130 mg, 0.18 mmol), and **15** (50 mg, 0.18 mmol) in dry DMF (20 mL) was stirred at room temperature for 14 d. The solvent was removed under reduced pressure, and the residue was purified by column chromatography (SiO_2, MeOH/2 M NH_4Cl_{aq}/$MeNO_2$, 7:2:1). The red fractions were combined, and the solvent was removed under vacuum. The red residue was dissolved in H_2O (200 mL), and a saturated aqueous solution of NH_4PF_6 was added. The resulting precipitate was filtered off, washed with H_2O, and dissolved in MeCN. Vapor diffusion of *i*Pr_2O into the MeCN solution afforded the [2]catenane **16·4PF$_6$** (109 mg, 35%) as a red crystalline solid. M.p. 280 °C decomp; LSIMS: *m/z*: 1740 $[M-PF_6]^+$, 1595 $[M-2PF_6]^+$, 1450 $[M-3PF_6]^+$; HRMS (LSIMS): calcd for $[M-3PF_6]^+$ ($C_{70}H_{76}F_{12}N_6O_{10}P_2$): calcd 1450.4907, found 1450.4855; ^{1}H NMR (CD_3CN): $\delta = 9.18–9.13$ (m, 8H), 8.18–8.14 (m, 8H), 8.05 (s, 8H), 7.50–7.40 (m, 4H), 7.00–6.90 (m, 4H), 5.59 (s, 8H), 4.20–3.60 (m, 32H), 2.82 (s, 4H).

[2]Catenane 17·4PF$_6$: A solution of **13** (250 mg, 0.36 mmol), **14·2PF$_6$** (130 mg, 0.18 mmol), and **15** (50 mg, 0.18 mmol) in dry DMF (20 mL) was stirred at room temperature for 14 d. The solvent was removed under reduced pressure and the residue was purified by column chromatography (SiO_2, MeOH/2 M NH_4Cl_{aq}/$MeNO_2$, 7:2:1). The purple fractions were combined, and the solvent was removed under vacuum. The purple residue was dissolved in H_2O (200 mL), and a saturated aqueous solution of NH_4PF_6 was added. The resulting precipitate was filtered off, washed with H_2O, and dissolved in MeCN. Vapor diffusion of *i*Pr_2O into the MeCN solution afforded the [2]catenane **17·4PF$_6$** (119 mg, 37%) as a purple crystalline solid. M.p. 280 °C decomp; LSIMS: *m/z*: 1645 $[M-PF_6]^+$, 1500 $[M-2PF_6]^+$, 1373 $[M-3PF_6]^+$; HRMS (LSIMS): calcd for $[M-PF_6]^+$ ($C_{74}H_{78}F_{18}N_6O_{10}P_3$) 1645.4705, found 1645.4736; ^{1}H NMR ($(CD_3)_2CO$): $\delta =$ 9.18–9.05 (m, 4H), 9.04–8.95 (m, 4H), 8.41–8.25 (bm, 4H), 8.15–8.05 (m, 4H), 7.65–7.52 (m, 4H), 7.51–7.48 (m, 4H), 7.41–7.30 (m, 4H), 6.90–6.82 (m, 4H), 6.35–6.25 (m, 2H), 6.18–6.03 (m, 2H), 5.89 (s, 8H), 4.45–4.34 (m, 4H), 4.28–4.20 (m, 4H), 4.19–4.10 (m, 4H), 4.09–4.03 (m, 4H), 4.03–3.92 (m, 4H), 3.90–3.80 (m, 8H), 3.79–3.71 (m, 4H), 2.66–2.2.55 (m, 2H). Single crystals suitable for X-ray crystallographic analysis were grown by vapor diffusion of PhH into a MeCN solution of **17·4PF$_6$**.

4,4′-Bis{2-{2-[2-(2-hydroxyethoxy)ethoxy]ethoxy}ethoxy}azobenzene (19): A solution of **6** (5.71 g, 27 mmol) and **18** (18.60 g, 51 mmol) in dry MeCN (200 mL), containing K_2CO_3 (14.60 g, 106 mmol) and catalytic amounts of LiBr, was heated under reflux and an atmosphere of N_2 for 4 d. The mixture was filtered while hot, and the solid residue was washed with MeCN. The combined organic solutions were concentrated under reduced pressure, and the residue was dissolved in CH_2Cl_2 (100 mL), washed with H_2O (100 mL), brine (5 × 100 mL), and dried ($MgSO_4$). The solvent was removed under vacuum, and the residue was crystallized from hexane/$CHCl_3$ (60:40) to afford **18** (12.23 g, 75%) as an orange solid. M.p. 36–38 °C; LSIMS: *m/z*: 567 $[M+H]^+$; HRMS (LSMS): calcd for $[M+H]^+$ ($C_{28}H_{43}N_2O_{10}$) 567.2907, found 567.2918; ^{1}H NMR ($CDCl_3$): $\delta = 7.89–7.80$ (m, 4H), 7.03–6.95 (m, 4H), 4.25–4.15 (m, 4H), 3.90–3.80 (m, 4H), 3.71–3.66 (m, 24H), 2.51–2.45 (m, 2H); ^{13}C NMR ($CDCl_3$): $\delta = 160.8, 147.2, 124.3, 114.9, 72.5, 70.9, 70.7, 70.6, 70.4, 69.7, 67.7, 61.8$.

4,4′-Bis{2-{2-[2-(2-tosyloxyethoxy)ethoxy]ethoxy}ethoxy}azobenzene (20): A solution of *p*-toluensulfonyl chloride (3.81 g, 20 mmol) in THF (40 mL) was added dropwise over 1 h to a solution of **19** (5.00 g, 9 mmol) and NaOH (1.00 g, 25 mmol) in THF (170 mL) and H_2O (170 mL) maintained at −5 °C. The mixture was stirred for further 24 h at −5 °C and then was diluted with cold H_2O (200 mL) and washed with $CHCl_3$ (3 × 100 mL). The organic layer was dried ($MgSO_4$) and concentrated under vacuum to afford a solid residue, which was crystallized twice from hexane/CH_2Cl_2 (60:40) to give **20** (7.12 g, 97%) as an orange solid. M.p. 42–45 °C; LSIMS: *m/z*: 875 $[M]^+$; ^{1}H NMR ($CDCl_3$): $\delta = 7.92–7.84$ (m, 4H), 7.82–7.73 (m, 4H), 7.38–7.30 (m, 4H), 7.03–6.97 (m, 4H), 4.25–4.15 (m, 8H), 3.80–3.65 (m, 24H), 2.45 (s, 6H); ^{13}C NMR ($CDCl_3$): $\delta = 147.2, 129.8, 127.8, 124.3, 114.8, 70.9, 70.7, 70.6, 69.7, 69.3, 68.7, 67.7, 21.7$.

4,4′-Azophenyl-*p*-phenylene-*p*-phenylene-57-crown-15 (22): A solution of **20** (7.86 g, 9 mmol) in dry DMF (300 mL) was added dropwise over 4 h to a solution of **21** (3.55 g, 9 mmol) in dry DMF (300 mL), containing Cs_2CO_3 (68.15 g, 209 mmol) and CsOTs (6.82 g, 22 mmol), maintained at 70 °C under an atmosphere of N_2. The temperature was raised to 80 °C, and the mixture was stirred for further 7 d and then filtered while hot. The solid residue was washed with $CHCl_3$ (300 mL), and the solvent of the combined organic solutions was removed under vacuum. The residue was dissolved in $CHCl_3$ (150 mL) and washed with H_2O (150 mL). The aqueous layer was extracted with $CHCl_3$ (4 × 100 mL), and the organic solutions were combined and dried ($MgSO_4$). The solvent was removed under reduced pressure, and the residue purified by column chromatography (SiO_2, $Et_2O/CHCl_3$/MeOH, 69:30:1) to afford **22** (390 mg, 5%) as a yellow oil. LSIMS: *m/z*: 908 $[M]^+$; HRMS (LSIMS): calcd for $[M]^+$ ($C_{48}H_{68}N_2O_{15}$) 909.4385, found 909.4378; ^{1}H NMR ($CDCl_3$): $\delta = 7.92–7.85$ (m, 4H), 7.32–6.72 (m, 4H), 6.75 (s, 8H), 4.15–3.65 (m, 48H); ^{13}C NMR (CD_3CN): $\delta = 153.1, 124.3, 115.6, 114.8, 70.8, 69.8, 69.6, 68.1, 67.8$.

[2]Catenane 23·4PF$_6$: A solution of **22** (100.0 mg, 0.11 mmol), **14·2PF$_6$** (77.8 mg, 0.11 mmol), and **15** (29.0 mg, 0.11 mmol) in dry DMF (20 mL) was stirred at room temperature for 14 d. The solvent was removed under reduced pressure, and the residue was purified by column chromatography (SiO_2, MeOH/2 M NH_4Cl_{aq}/$MeNO_2$, 7:2:1). The red fractions were combined, and the solvent was removed under vacuum. The red residue was dissolved in H_2O (200 mL), and a saturated aqueous solution of NH_4PF_6 was added. The resulting precipitate was filtered off, washed with H_2O, and dissolved in MeCN. Vapor diffusion of *i*Pr_2O into the MeCN solution afforded the [2]catenane **17·4PF$_6$** (66 mg, 30%) as a red crystalline solid. M.p. 280 °C decomp; LSIMS: *m/z*: 2009 $[M]^+$, 1864 $[M-PF_6]^+$, 1719 $[M-2PF_6]^+$, 1574 $[M-3PF_6]^+$; HRMS (LSIMS): calcd for $[M-PF_6]^+$ ($C_{84}H_{96}F_{18}N_6O_{15}P_3$) 1863.5859, found 1863.5868; ^{1}H NMR ($(CD_3)_2CO$, 253 K): $\delta = 9.38–9.25$ (m, 8H), 8.28–8.15 (bs, 8H), 8.00 (s, 4H), 7.91 (s, 4H), 7.75–7.71 (m, 2H), 7.35–7.29 (m, 2H), 7.15–7.04 (m, 2H), 6.70–6.60 (m, 2H), 6.58–6.54 (m, 2H), 6.45–6.35 (m, 2H), 6.03–5.81 (m, 8H), 4.21–3.44 (m, 52H).

1,4-Bis{2-[2-(2-hydroxyethoxy)ethoxy]ethoxy}benzenemonotosylate (25): A solution of *p*-toluensulfonyl chloride (1.13 g, 56 mmol) was added dropwise over 1 h to a solution of **24** (8.00 g, 16 mmol) and NaOH (1.04 g, 26 mmol) in THF (200 mL) and H_2O (25 mL) maintained at −5 °C. The mixture was stirred for further 2 h at −5 °C, poured into ice/H_2O (50 mL), and washed with CH_2Cl_2 (3 × 100 mL). The organic layer was dried ($MgSO_4$) and concentrated under vacuum. The resulting oil was purified by column chromatography (SiO_2, CH_2Cl_2/MeOH, 100:2) to afford **25** (1.68 g, 20%) as a colorless oil. LSIMS: *m/z*: 528 $[M]^+$; ^{1}H NMR ($CDCl_3$): $\delta =$ 7.78–7.70 (m, 2H), 7.29–7.22 (m, 2H), 6.65 (s, 4H), 4.15–4.10 (m, 2H), 4.05–3.95 (m, 4H), 3.80–3.50 (m, 22H), 2.43 (s, 3H); ^{13}C NMR ($CDCl_3$): $\delta = 153.0, 144.8, 133.0, 129.9, 128.0, 115.6, 72.5, 70.8, 70.3, 69.9, 69.3, 68.7, 68.0, 61.7, 21.6$.

2-{2-{2-{4-{2-{2-[2-(4-Triphenylmethylphenoxy)ethoxy]ethoxy}ethoxy}phenoxy}ethoxy}ethoxy}ethanol (27): A solution of **25** (2.00 g, 4 mmol) and **26** (1.40 g, 4 mmol) in dry MeCN (200 mL), containing K_2CO_3 (8.00 g, 60,0 mmol) and catalytic amounts of LiBr, was heated under reflux and an atmosphere of N_2 for 24 h. After cooling down to room temperature, the mixture was filtered, and the solid residue was dissolved in H_2O and washed with CH_2Cl_2 (2 × 50 mL). The combined organic solutions were concentrated under reduced pressure. The resulting residue was dissolved in CH_2Cl_2 (200 mL), washed with 10% aqueous NaOH (3 × 100 mL), and dried ($MgSO_4$). The solvent was removed under vacuum, and the resulting solid was crystallized from CH_2Cl_2 to afford **27** (2.09 g, 70%) as a white solid. LSIMS: *m/z*: 692 $[M]^+$; ^{1}H NMR ($CDCl_3$): $\delta = 7.25–7.15$ (m, 15H), 7.13–7.06 (m, 2H), 6.85 (s, 4H), 6.78–6.72 (m, 2H), 4.18–4.03 (m, 6H), 3.90–3.80 (m, 6H), 3.75–3.52 (m, 12H); ^{13}C NMR ($CDCl_3$): $\delta = 147.0, 132.2, 131.1, 127.4, 125.8, 115.6, 113.4, 72.5, 70.9, 70.4, 69.9, 68.0, 67.3, 61.8$.

2-{2-{2-{4-{2-{2-[2-(4-Triphenylmethylphenoxy)ethoxy]ethoxy}ethoxy}phenoxy}ethoxy}ethoxy}ethanoltosylate (28): A solution of *p*-toluenesulfonyl chloride (1.13 g, 6 mmol) in THF (25 mL) was added dropwise over 1 h to a solution of **27** (2.24 g, 3 mmol) and NaOH (0.15 g, 4 mmol) in THF (30 mL) and H_2O (25 mL) maintained at −5 °C. The mixture was stirred for a

0947-6539/99/0503-0872 $ 17.50+.50/0 *Chem. Eur. J.* **1999**, *5*, No. 3

further 2 h at −5 °C, poured into ice/H_2O (50 mL) and washed with CH_2Cl_2 (3 × 100 mL). The organic layer was dried ($MgSO_4$) and concentrated under reduced pressure. The resulting oil was purified by column chromatography (SiO_2, CH_2Cl_2/MeOH, 100:2) to afford **28** (6.71 g, 80 %) as a colorless oil. LSIMS: *m/z*: 846 $[M+H]^+$; ^{1}H NMR ($CDCl_3$): δ = 7.88–7.83 (m, 2H), 7.38–6.75 (m, 25H), 4.25–4.01 (m, 8H), 3.92–3.61 (m, 16H), 2.45 (s, 3H); ^{13}C NMR ($CDCl_3$): δ = 156.8, 153.1, 147.1, 144.9, 139.2, 132.2, 131.2, 129.9, 128.0, 127.5, 125.9, 115.6, 113.4, 70.9, 70.0, 69.8, 69.4, 68.8, 68.0, 67.3, 21.7.

4,4′-Bis{2-{2-{2-{4-{2-{2-[2-(4-Triphenylmethylphenoxy)ethoxy]ethoxy}ethoxy}phenoxy}ethoxy}ethoxy}ethoxy}azobenzene (**29**): A solution of **28** (1.70 g, 2 mmol) in dry THF (200 mL) was added dropwise over 1 h to a solution of **6** (0.22 g, 1 mmol) and NaH (48 mg, 2 mmol) in dry THF (250 mL) maintained at 60 °C under an atmosphere of N_2. The mixture was heated under reflux for a further 2 days. After cooling down to room temperature, H_2O (10 mL) was added, and the solvent was removed under vacuum. The residue was purified by column chromatography (SiO_2, CH_2Cl_2/MeOH, 100:2) to afford **29** (0.24 g, 15 %) after crystallization from hexane/CH_2Cl_2 (60:40). LSIMS: *m/z*: 1564 $[M]^+$; HRMS (LSIMS) $[M+H]^+$ ($C_{98}H_{103}N_2O_{16}$): calcd 1563.7308, found 1563.7262; ^{1}H NMR ($CDCl_3$): δ = 7.50–6.70 (m, 54H), 4.15–3.61 (m, 48H); ^{13}C NMR ($CDCl_3$): δ = 160.8, 156.7, 153.1, 147.0, 139.2, 132.2, 131.1, 127.5, 125.9, 124.4, 115.6, 114.8, 113.4, 72.6, 71.4, 70.9, 70.0, 69.8, 68.0, 67.7, 67.3, 64.3, 56.2, 42.8.

[2]Rotaxane 30·4PF_6

Method A: A solution of **29** (100 mg, 0.06 mmol), **14**·2PF_6 (50.0 mg, 0.07 mmol), and **15** (20.0 mg, 0.07 mmol) in dry DMF was stirred at room temperature for 14 d. The solvent was removed under reduced pressure, and the residue was purified by column chromatography (SiO_2, MeOH/2 M NH_4Cl_{aq}/$MeNO_2$, 7:2:1). The red fractions were combined and the solvent was removed under vacuum. The red residue was dissolved in H_2O (200 mL), and a saturated aqueous solution of NH_4PF_6 was added. The resulting precipitate was filtered off, washed with H_2O, and dried to afford the [2]rotaxane **30**·4PF_6 (4 mg, 2 %) as a red solid. M.p. 280 °C decomp; LSIMS: *m/z*: 2519 $[M-PF_6]^+$, 2374 $[M-2PF_6]^+$, 2229 $[M-3PF_6]^+$; HRMS (LSIMS) $[M-2PF_6]^+$ ($C_{134}H_{134}F_{12}N_6O_{16}P_2$): calcd 2372.9103, found 2372.9140; ^{1}H NMR ($(CD_3)_2CO$, 235 K): δ = 9.35–9.45 (m, 4H), 9.24–9.15 (m, 4H), 8.25–8.20 (m, 4H), 8.10–8.05(m, 4H), 7.95 (s, 8H), 7.75–7.69 (m, 4H), 7.49–7.45 (m, 4H), 7.28–7.06 (m, 30H), 7.08–7.02 (m, 2H), 7.05–6.98 (m, 2H), 6.88–6.83 (m, 2H), 6.82–6.77 (m, 2H), 6.77–6.70, (m, 2H), 6.57–6.48 (m, 2H), 6.45–6.38 (m, 2H), 4.35–3.96 (m, 48H).

Method B: A solution of **29** (100.0 mg. 0.06 mmol), **14**·2PF_6 (50.0 mg, 0.07 mmol), and **15** (20.0 mg, 0.07 mmol) in dry DMF was subjected to a pressure of 12 kbar at room temperature for 4 d. The solvent was removed under reduced pressure and the residue was purified by column chromatography (SiO_2, MeOH/2 M NH_4Cl_{aq}/$MeNO_2$, 7:2:1). The red fractions were combined, and the solvent was removed under vacuum. The red residue was dissolved in H_2O (200 mL), and a saturated aqueous solution of NH_4PF_6 was added. The resulting precipitate was filtered off, washed with H_2O, and dried to afford the [2]rotaxane **30**·4PF_6 (39 mg, 21 %) as a red solid.

X-ray crystallography: Table 3 provides a summary of the crystal data, data collection, and refinement parameters for the complex [**1**:**8**]·4PF_6, the macrocyclic polyether **13**, and the [2]catenane **17**·4PF_6. The structures were solved by direct methods and were refined by full matrix least-squares based on F^2 (blocked in the case **17**·4PF_6). In the complex [**1**:**8**]·4PF_6, the guest was found to be disordered over the crystallographic center of symmetry and was modeled by the use of one complete, half-occupancy but off-set guest, the non-hydrogen atoms of which were refined isotropically. In the macrocyclic polyether **13**, part of one of the polyether chains was found to be disordered and was resolved in two partial occupancy orientations with the non-hydrogen atoms of the major occupancy orientation being refined anisotropically. The disorder found in the macrocyclic polyether component of the [2]catenane **17**·4PF_6 was more extensive with the 4,4′-azobiphenoxy unit being disordered. This disorder was resolved into two half-occupancy *trans* orientations (related by an approximate C_2 flip about the [O···O] vector), both of which were refined isotropically. In the complex [**1**:**8**]·4PF_6 and in the [2]catenane **17**·4PF_6, disorder was found in one of the hexafluorophosphate anions and in each case it was resolved into two partial occupancy orientations with only the major occupancy atoms being refined anisotropically. The hydrate molecules in [**1**:**8**]·4PF_6 were found to be distributed over two half-occupancy sites, the oxygen atoms of both of which were refined isotropically. The included MeCN molecules in [**1**:**9**]·4PF_6 were found to be distributed over one full and four half-occupancy sites, the non-hydrogen atoms of all of which were refined anisotropically. The remaining non-hydrogen atoms in

Table 3. Crystal data, data collection, and refinement parameters for the complex [**1**:**8**]·4PF_6, the macrocyclic polyether **13**, and the [2]catenane **17**·4PF_6.[a]

	[**1**:**8**]·4PF_6	**13**	**17**·4PF_6
formula	$C_{56}H_{58}N_6O_6\cdot 4PF_6$	$C_{38}H_{46}N_2$	$C_{74}H_{78}N_6O_{10}\cdot 4PF_6$
solvent	2MeCN·2H_2O	–	PhH·3MeCN
formula weight	1609.1	690.8	1922.6
color, habit	red prisms	yellow rhombs	red rhombs
crystal size [mm]	1.00 × 0.67 × 0.33	0.67 × 0.57 × 0.40	1.00 × 0.73 × 0.43
crystal system	monoclinic	triclinic	monoclinic
space group	$P2_1/n$ (No. 14)	$P\bar{1}$ (No. 2)	$C2/c$ (No. 15)
a [Å]	11.639(4)	10.459(1)	62.245(3)
b [Å]	17.832(3)	12.259(1)	13.508(1)
c [Å]	17.726(3)	14.176(2)	23.297(1)
α [°]	–	82.09(1)	–
β [°]	98.62(2)	84.21(1)	92.94(1)
γ [°]	–	86.62(1)	–
V [Å^3]	3638(2)	1789.2(3)	19562(2)
Z	2[b]	2	8
ρ_{calcd} [g cm^{-3}]	1.469	1.282	1.353
$F(000)$	1648	736	8224
radiation used	$Mo_{K\alpha}$	$Mo_{K\alpha}$	$Cu_{K\alpha}$
μ [mm^{-1}]	0.22	0.09	1.63
θ range [deg]	2.0–23.0	2.0–24.0	2.8–55.0
reflections measured	5011	5585	12254
reflections observed, $\lvert F_o\rvert > 4\sigma(\lvert F_o\rvert)$	3365	4146	6950
parameters	455	460	1290
R_1[c]	0.155	0.048	0.111
wR_2[d]	0.433	0.125	0.300
weighting factors a, b[e]	0.208, 21.978	0.062, 0.549	0.239, 6.146
largest diff. peak, hole [e Å^{-3}]	0.81, −0.37	0.35, −0.18	0.69, −0.38

[a] Details in common: graphite monochromated radiation, ω-scans, Siemens P4/PC diffractometer, 293 K, refinement based on F^2. [b] The molecule has crystallographic C_i symmetry. [c] $R_1 = \Sigma\,||F_o| - |F_c||/\Sigma\,|F_o|$. [d] $wR_2 = [\Sigma w(F_o^2 - F_c^2)^2/\Sigma w(F_o^2)^2]^{1/2}$. [e] $w^{-2} = \sigma^2(F_o^2) + (aP)^2 + bP$.

all of the structures were refined anisotropically. In each structure the C–H hydrogen atoms were placed in calculated positions, assigned isotropic thermal parameters, $U(H) = 1.2\,U_{eq}(C)$ [$U(H) = 1.5\,U_{eq}(C\text{–}Me)$], and allowed to ride on their parent atoms. The O–H hydrogen atoms in [**1**:**8**]·$4PF_6$ could not be located. Computations were carried out with the SHELXTL PC program system.[22] Crystallographic data (excluding structure factors) for the structures reported in this paper have been deposited with the Cambridge Crystallographic Data Centre as supplementary publication no. CCDC-101867 – 101869. Copies of the data can be obtained free of charge on application to CCDC, 12 Union Road, Cambridge CB21EZ, UK (fax: (+44) 1223-336-033; e-mail: deposit@ccdc.cam.ac.uk).

Absorption and luminescence spectra: Experimental procedures and equipment have been previously described.[11b, 13] Correction of the luminescence intensity for inner filter effects was performed when necessary.[23] Experimental errors: absorption and emission maxima, ±2 nm; luminescence quantum yields, ±15%; luminescence lifetimes, ±10%.

Photochemistry: Photochemical experiments were carried out in a 1 cm thick spectrofluorimetric cell on air-equilibrated 5×10^{-5} M MeCN solutions at room temperature with a medium pressure Q400 Hanau mercury lamp. The irradiation wavelengths, 287 nm, 365 nm, and 436 nm, were isolated by means of interference filters. The incident-light intensity, determined by ferrioxalate actinometry,[24] was of the order of 1×10^{-7} Nh$\tilde{\nu}$min^{-1}. The values of $\Phi_{t\rightarrow c}$ were measured by irradiating a solution of the pure *trans* isomer; its disapperance was followed through absorbance measurements at 355 nm, at which the *cis* form, to all intents and purposes, does not absorb. The photostationary state obtained with 365 nm irradiation contains about 95% of the *cis* isomer. The *cis* → *trans* photoisomerization studies were performed starting from such a photostationary state. The values of $\Phi_{c\rightarrow t}$ were measured by evaluating the appearance of the absorbance signal of the *trans* isomer at 355 nm. When necessary, corrections were made for the fraction of light absorbed at the irradiation wavelength. In all quantum yield determinations, irradiation was such that no more than 10% isomerization was achieved. The experimental error on the quantum yields values is ±15%.

Acknowledgments

This research was supported by the Engineering and Physical Sciences Research Council in the United Kingdom and by the University of Bologna (Funds for Selected Research Topics) and MURST in Italy, and by the EU (TMR grant FMRX-CT96-0076).

[1] a) H. Rau, *Photochromism: Molecules and Systems* (Eds.: H. Dürr, H. Bouas-Laurent), Elsevier, Amsterdam, **1990**, pp. 165 – 192; b) B. L. Feringa, W. F. Jager, B. de Lange, *Tetrahedron* **1993**, *49*, 8267 – 8310.

[2] a) V. Balzani, F. Scandola, *Supramolecular Photochemistry*, Horwood, Chichester, **1991**; b) V. Balzani, *Tetrahedron* **1992**, *48*, 10443 – 10514; c) V. Balzani, M. Gopéz-Lopéz, J. F. Stoddart, *Acc. Chem. Res.* **1998**, *31*, 405 – 414; d) R. A. Bissell, A. P. de Silva, H. Q. N. Gunaratne, P. L. M. Lynch, G. E. M. Maguire, K. R. A. S. Sandanayake, *Chem. Soc. Rev.* **1992**, *21*, 187 – 195; e) R. A. Bissell, A. P. de Silva, H. Q. N. Gunaratne, P. L. M. Lynch, G. E. M. Maguire, C. P. McCoy, K. R. A. S. Sandanayake, *Top. Curr. Chem.* **1993**, *168*, 223 – 264; f) A. P. de Silva, C. P. McCoy, *Chem. Ind.* **1994**, 992 – 996; g) A. P. de Silva, H. Q. N. Gunaratne, T. Gunnlaugsson, A. J. M. Huxley, C. P. McCoy, J. T. Rademacher, T. E. Rice, *Chem. Rev.* **1997,** *97*, 1515 – 1566; h) P. D. Beer, *Adv. Inorg. Chem.* **1992**, *39*, 79 – 157; i) P. D. Beer, *Adv. Mater.* **1994**, *6*, 607 – 609; j) P. D. Beer, *Chem. Commun.* **1996**, 689 – 696; k) L. Fabbrizzi, A. Poggi, *Chem. Soc. Rev.* **1995**, *24*, 197 – 202; l) M. D. Ward, *Chem. Ind.* **1997**, 640 – 645.

[3] For reviews on azobenzene-based systems, see: a) S. Shinkai, O. Manabe, *Top. Curr. Chem*. **1984**, *121*, 76 – 104; b) F. Vögtle, *Supramolecular Chemistry*, Wiley, New York, **1991**, chapter 7; c) J. I. Anzai, T. Osa, *Tetrahedron* **1994**, *50* , 4039 – 4070.

[4] R. Gillard, F. M. Raymo, J. F. Stoddart, *Chem. Eur. J.* **1997**, *3*, 1933 – 1940.

[5] For examples of chemically-, electrochemically-, and/or photochemically-controllable mechanically interlocked molecules, see: a) A. Livoreil, C. O. Dietrich-Buchecker, J.-P. Sauvage, *J. Am. Chem. Soc.* **1994**, *116*, 9399 – 9400; b) D. B. Amabilino, C. O. Dietrich-Buchecker, A. Livoreil, L. Pérez-García, J.-P. Sauvage, J. F. Stoddart, *J. Am. Chem. Soc.* **1996**, *118*, 3905 – 3913; c) D. J. Cárdenas, A. Livoreil, J.-P. Sauvage, *J. Am. Chem. Soc.* **1996**, *118*, 11980 – 11981; d) F. Baumann, A. Livoreil, W. Kaim, J.-P. Sauvage, *Chem. Commun.* **1997**, 35 – 36; e) A. Livoreil, J.-P. Sauvage, N. Armaroli, V. Balzani, L. Flamigni, B. Ventura, *J. Am. Chem. Soc.* **1997**, *119*, 12114 – 12124; f) A. C. Benniston, A. Harriman, *Angew. Chem.* **1993**, *105*, 1553 – 1555; *Angew. Chem. Int. Ed. Engl.* **1993**, *32*, 1459 – 1461; g) A. C. Benniston, A. Harriman, D. Philp, J. F. Stoddart, *J. Am. Chem. Soc.* **1993**, *115*, 5298 – 5299; h) A. C. Benniston, A. Harriman, V. M. Lynch, *Tetrahedron Lett.* **1994**, *35*, 1473 – 1476; i) A. C. Benniston, A. Harriman, V. M. Lynch, *J. Am. Chem. Soc.* **1995**, *117*, 5275 – 5291; j) A. C. Benniston, *Chem. Soc. Rev.* **1996**, *25*, 427 – 435; k) A. C. Benniston, A. Harriman, D. S. Yufit, *Angew. Chem.* **1997**, *109*, 2451 – 2454; *Angew. Chem. Int. Ed. Engl.* **1997**, *36*, 2356 – 2358; l) R. Ballardini, V. Balzani, M. T. Gandolfi, L. Prodi, M. Venturi, D. Philp, H. G. Ricketts, J. F. Stoddart, *Angew. Chem.* **1993**, *105*, 1362 – 1364; *Angew. Chem. Int. Ed. Engl.* **1993**, *32*, 1301 – 1303; m) R. A. Bissell, E. Córdova, A. E. Kaifer, J. F. Stoddart, *Nature* **1994**, *369*, 133 – 137; n) R. Ballardini, V. Balzani, A. Credi, M. T. Gandolfi, S. J. Langford, S. Menzer, L. Prodi, J. F. Stoddart, M. Venturi, D. J. Williams, *Angew. Chem.* **1996**, *108*, 1056 – 1059; *Angew. Chem. Int. Ed. Engl.* **1996**, *35*, 978 – 981; o) M.-V. Martínez-Díaz, N. Spencer, J. F. Stoddart, *Angew. Chem.* **1997**, *109*, 1991 – 1994; *Angew. Chem. Int. Ed. Engl.* **1997**, *36*, 1904 – 1907; p) P.-L. Anelli, M. Asakawa, P. R. Ashton, R. A. Bissell, G. Clavier, R. Górski, A. E. Kaifer, S. J. Langford, G. Mattersteig, S. Menzer, D. Philp, A. M. Z. Slawin, N. Spencer, J. F. Stoddart, M. S. Tolley, D. J. Williams, *Chem. Eur. J.* **1997**, *3*, 1113 – 1135; q) M. Asakawa, P. R. Ashton, V. Balzani, A. Credi, G. Mattersteig, O. A. Matthews, M. Montalti, N. Spencer, J. F. Stoddart, M. Venturi, *Chem. Eur. J.* **1997**, *3*, 1992 – 1996; r) A. Credi, V. Balzani, S. J. Langford, J. F. Stoddart, *J. Am. Chem. Soc.* **1997**, *119*, 2679 – 2681; s) P. R. Ashton, R. Ballardini, V. Balzani, M. Gómez-López, S. E. Lawrence, M.-V. Martínez-Díaz, M. Montalti, A. Piersanti, L. Prodi, J. F. Stoddart, D. J. Williams, *J. Am. Chem. Soc.* **1997**, *119*, 10641 – 10651; t) M. Asakawa, P. R. Ashton, V. Balzani, A. Credi, C. Hamers, G. Mattersteig, M. Montalti, A. N. Shipway, N. Spencer, J. F. Stoddart, M. S. Tolley, M. Venturi, A. J. P. White, D. J. Williams, *Angew. Chem.* **1998**, *110*, 357 – 361; *Angew. Chem. Int. Ed.* **1998**, *37*, 333 – 337; u) O. A. Matthews, F. M. Raymo, J. F. Stoddart, A. J. P. White, D. J. Williams, *New J. Chem.* **1998**, 1131 – 1134; v) P. R. Ashton, V. Balzani, O. Kocian, L. Prodi, N. Spencer, J. F. Stoddart, *J. Am. Chem. Soc.* **1998**, *120*, 11190 – 11191; w) P. R. Ashton, R. Ballardini, V. Balzani, I. Baxter, A. Credi, M. C. T. Fyfe, M. T. Gandolfi, M. Gómez-López, M.-V. Martínez-Díaz, A. Piersanti, N. Spencer, J. F. Stoddart, M. Venturi, A. J. P. White, D. J. Williams, *J. Am. Chem. Soc.* **1998**, *120*, 11932 – 11942.

[6] For azobenzene-containing catenanes and rotaxanes, see: a) F. Vögtle, W. M. Müller, U. Müller, M. Bauer, K. Rissanen, *Angew. Chem.* **1993**, *105*, 1356 – 1358; *Angew. Chem. Int. Ed. Engl.* **1993**, *32*, 1295 – 1297; b) M. Bauer, W. M. Müller, U. Müller, K. Rissanen, F. Vögtle, *Liebigs Ann.* **1995**, 649 – 656; c) H. Murakami, A. Kawabuchi, K. Kotoo, M. Kunitake, N. Nakashima, *J. Am. Chem. Soc.* **1997**, *119*, 7605 – 7606.

[7] The liquid secondary ion mass spectra (LSIMS) of equimolar mixtures of **1**·$4PF_6$ and *trans*-**9** or *trans*-**10** show peaks at *m/z* values for $[M - PF_6]^+$, $[M - 2PF_6]^+$, and $[M - 3PF_6]^+$ corresponding to the losses of one, two, and three hexafluorophosphate counterions, respectively, from the 1:1 complexes.

[8] This resonance was assigned to the aromatic protons of the *cis* isomer on the basis of a C–H correlation (gradient phase sensitive HSQC) NMR experiment.

[9] By employing the approximate coalescence treatment, a free energy barrier ($\Delta G_c^{\neq}$) of 14.6 ± 0.2 kcal mol^{-1} was determined for the shuttling process at a coalescence temperature (T_c) of 304 K. For a discussion of the approximate coalescence method, see: I. O. Sutherland *Annu. Rep. NMR Spectrosc.* **1971**, *4*, 71 – 73.

[10] H. Rau, *Angew. Chem.* **1973**, *85*, 248 – 258; *Angew. Chem. Int. Ed. Engl.* **1973**, *12*, 224 – 235.

[11] a) P.-L. Anelli, P. R. Ashton, R. Ballardini, V. Balzani, M. Delgado, M. T. Gandolfi, T. T. Goodnow, A. E. Kaifer, D. Philp, M. Pietraszkiewicz, L. Prodi, M. V. Reddington, A. M. Z. Slawin, N. Spencer, J. F.

  0947-6539/99/0503-0874 $ 17.50+.50/0

Stoddart, C. Vicent, D. J. Williams, *J. Am. Chem. Soc.* **1992**, *114*, 193–218; b) P. R. Ashton, R. Ballardini, V. Balzani, A. Credi, M. T. Gandolfi, S. Menzer, L. Pérez-García, L. Prodi, J. F. Stoddart, M. Venturi, A. J. P. White, D. J. Williams, *J. Am. Chem. Soc.* **1995**, *117*, 11171–11197.

[12] P. R. Ashton, R. Ballardini, V. Balzani, S. E. Boyd, A. Credi, M. T. Gandolfi, M. Gómez-López, S. Iqbal, D. Philp, J. A. Preece, L. Prodi, H. G. Ricketts, J. F. Stoddart, M. S. Tolley, M. Venturi, A. J. P. White, D. J. Williams, *Chem. Eur. J.* **1997**, *3*, 152–170.

[13] D. B. Amabilino, P. R. Ashton, V. Balzani, C. L. Brown, A. Credi, J. M. J. Fréchet, J. W. Leon, F. M. Raymo, N. Spencer, J. F. Stoddart, M. Venturi, *J. Am. Chem. Soc.* **1996**, *118*, 12012–12020.

[14] The rate constant of the energy-transfer quenching processes has been evaluated by the use of Equation (1) in which I_0 and τ_0 are the

$$k_{en} = \frac{1}{\tau_0}\left(\frac{I_0}{I} - 1\right) \quad (1)$$

fluorescence intensity and lifetime of the 1,5-dimethoxynaphthalene model compound, and I is fluorescence intensity of the macrocyclic polyether **13** under the same experimental and instrumental conditions.

[15] As can be seen from inspection of the data recorded in Table 2, the *trans* →*cis* photoisomerization quantum yield of **29** upon irradiation at 436 nm is considerably smaller than that of the other compounds. We have checked this value several times and we have no straightforward explanation for such strange behavior.

[16] D. D. Perrin, W. L. Armarego, *Purification of Laboratory Chemicals*, 3rd ed., Pergamon, New York, **1988**.

[17] M. Asakawa, W. Dehaen, G. L'abbé, S. Menzer, J. Nouwen, F. M. Raymo, J. F. Stoddart, D. J. Williams, *J. Org. Chem.* **1997**, *61*, 9561–9595.

[18] M. Ouchi, Y, Inoue, Y. Liu, S. Nagamura, S. Nakamura, K. Wada, T. Kakushi, *Bull. Chem. Soc. Jpn*. **1990**, *63*, 1260–1262.

[19] R. Willstätter, M. Benz, *Chem. Ber.* **1906**, *34*, 3492–3503.

[20] M. Asakawa, P. R. Ashton, S. E. Boyd, C. L. Brown, R. E. Gillard, O. Kocian, F. M. Raymo, J. F. Stoddart, M. S. Tolley, A. J. P. White, D. J. Williams, *J. Org. Chem.* **1997**, *62*, 26–37.

[21] B. Weickhardt, A. E. Siegrist, *Helv. Chim. Acta* **1972**, *55*, 138–172.

[22] *SHELXTL PC version 5.03*, Siemens Analytical X-Ray Instruments, Madison, WI, **1994**.

[23] A. Credi, L. Prodi, *Spectrochim. Acta A* **1998**, *54*, 159–170.

[24] a) C. G. Hatchard, C. A. Parker, *Proc. R. Soc. London A* **1956**, *235*, 518–536; b) E. Fisher, *EPA Newsletter* **1984**, July 3.

Received: June 9, 1998 [F1196]